TRACING THE EVOLUTION OF HIGHLY RESISTANT HIV-1 ENVELOPE PROTEINS

Jessy J. Duran Ramirez 15-706-609 and Jennifer Probst 16-703-423

jessyjomary.duranramirez@uzh.ch, jennifer.probst@uzh.ch

09.12.19

Table of contents

1. Abstract

The rapid evolution of HIV-1 viruses leads to quick escape from human immune pressures and has so far prevented successful vaccine development. In this report we aim to trace over time the evolution of viral envelope proteins in a patient. This was addressed by the generation of pseudoviruses expressing an envelope protein extracted from patient plasma over six different points in time. Subsequently, envelope functionality, antibody inhibition and genome sequence analysis where evaluated. Fitting to our hypothesis, we found infectious viruses to develop resistance against antibodies during disease progression. In line with these findings, envelope evolution was also observed on a genetic level, where two of the clones might have undergone a co-receptor switch.

We suggest a large-scale follow-up experiment testing co-receptor knockout/blocking and the comparison of mutations within different bnAb responses. In future, a deeper understanding of HIV-1 escape pathways will be crucial for effective vaccine design.

2. Introduction

The human immunodeficiency virus (HIV) is a Lentivirus belonging to the family of retroviruses (Freed, 2001) causing HIV infection in humans and subsequently in most cases the acquired immunodeficiency syndrome (AIDS), an ongoing condition of immune system failure. Two distinct types of HIV have been characterized. HIV-1, on which we focused here, is found throughout the world, whereas HIV-2 is mainly observed in western Africa (Reeves and Doms, 2002). HIV-1 was found to be more virulent and more infective than HIV-2 (Gilbert et al., 2003), also the likelihood of progression to AIDS was found to be higher (Nyamweya et al., 2013) and it is the cause of the majority of HIV infections globally (Reeves and Doms, 2002). The HIV-1 virus genome consists of two identical copies of a positive single stranded RNA and contains 9 open reading frames, producing 15 proteins (Coffin et al., 1997). It is approximately 861 amino acids long and encodes, among others, from the 5'- to 3'-ends for the gag (group-specific antigen), pol (polymerase) and env (envelope glycoprotein) genes (Freed, 2001). HIV is an enveloped virus, meaning that the viral capsid is surrounded by a membrane acquired during the budding from the host cell membrane. The envelope (env) gene encodes a 30 amino acid signal peptide (SP) and the two glycoproteins gp120 and gp41 (Watts et al., 2010), depicted in Figure 1.

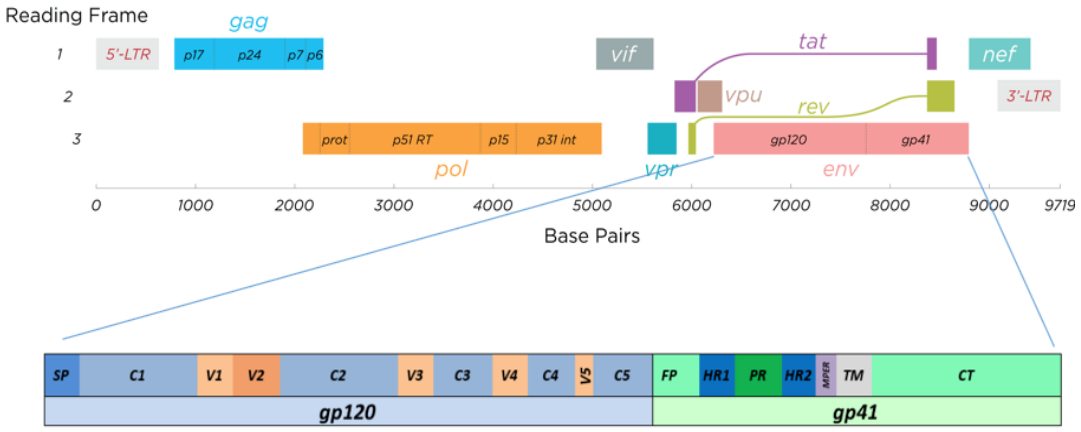

Figure 1: Overview of the full HIV-1 genome and a more detailed illustration of the envelope genome regions. The domains in gp120 from the beginning to the end are the signal peptide (SP), constant regions C1-C5, variable domains V1-V5. The domains in gp41 are the fusion peptide (FP), heptad repeats (HR) HR1 and HR2, the polar region (PR), the membrane proximal external region (MPER), the transmembrane region (TM) and the cytoplasmic tail (CT). The figure was modified from [3].

Glycoprotein spikes are incorporated into the envelope and represent the only viral protein on the lipid membrane surface. These envelope spikes are composed of three heterodimers each consisting of one transmembrane protein gp41 and one surface protein gp120 (Figure 2). These two viral envelope glycoproteins gp120 and gp41 are derived from a single gp160 poly-protein precursor (Figure 1). The gp160 protein is synthesised on the rough endoplasmic reticulum and arranged into trimers. After transportation to the Golgi, the protein gets heavily glycosylated to protect HIV from immune recognition (Joseph et al, 2018).

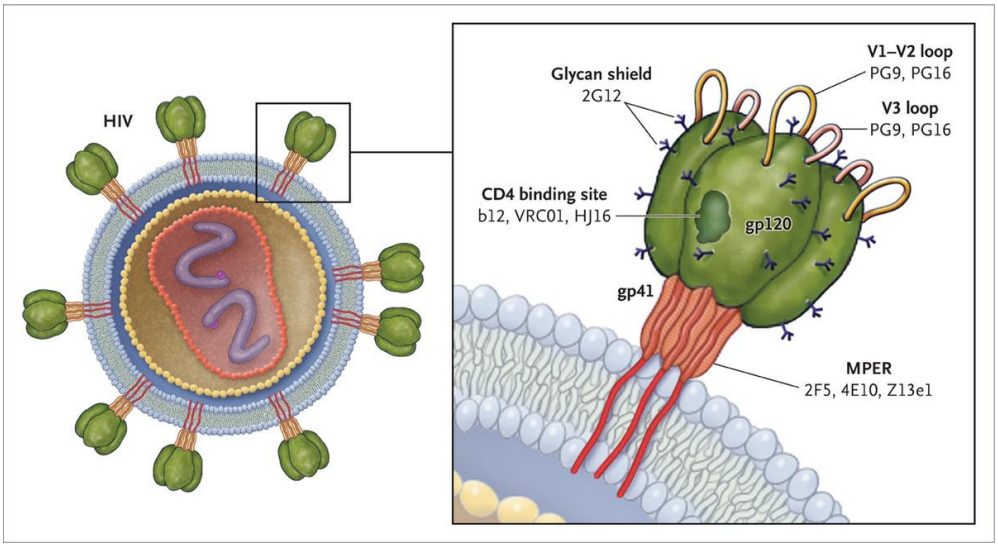

Figure 2: Illustration of an HIV virus, its envelope and the envelope glycoproteins. A) Schematic structure of the trimeric envelope spike. B) Envelope glycoprotein incorporated into the envelope with different epitopes for antibody targeting (V1-V2 loop, V3 loop, CD4 binding site, MPER). Figure taken from Koff and Berkley (2010).

The envelope spikes mediate the entry process of the virus into the host cell (Figure 3). HIV-1 specifically targets the CD4 positive T-lymphocytes in the peripheral blood. Therefore, gp120 is first used for attachment to on the CD4 receptor of the target cell (Freed, 2001). Upon successful binding to the T cell CD4 receptor, the envelope spike undergoes a conformational change and can in a second step bind a co-receptor in a second step. This initiates membrane fusion of virus and host cell, where the transmembrane protein gp41 is used to help the virus to fuse with the host cell membrane (Chan and Kim, 1998).

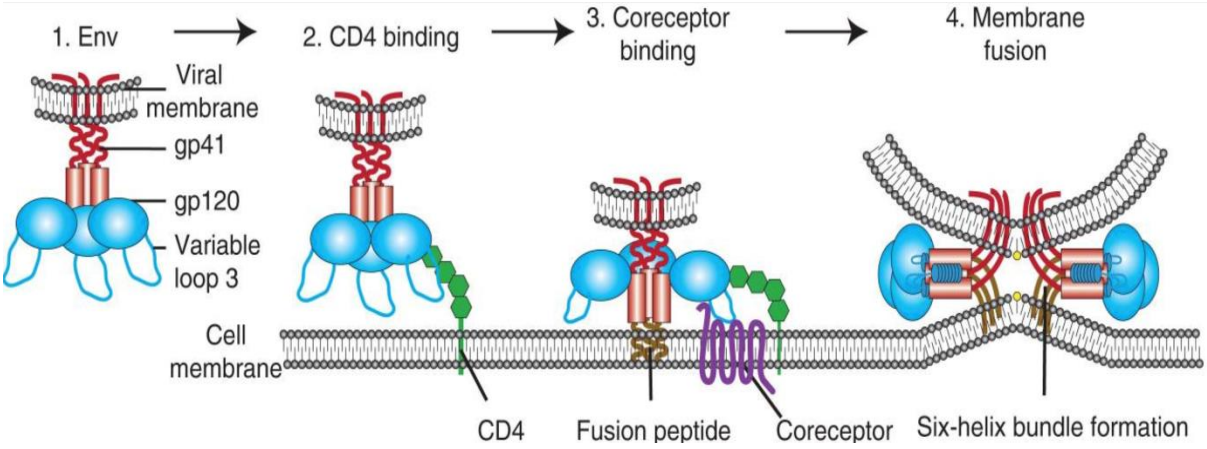

Figure 3: Overview of the entry process of HIV-1. CD4 is used as primary binding receptor, whereas the chemokine receptors CCR5 or CXCR4 serve as co-receptors. Figure taken from [4].

HIV-1 uses chemokine receptors as coreceptors, either CCR5 or CXCR4 or both. The viruses are classified according to co-receptor usage: R5 trophic if CCR5 is used, X4 trophic in the case for CXCR4 or dual trophic if both are utilized. At the beginning of an infection all transmitted viruses are R5 tropic. In about 50% of all infected patients the HIV viruses switch to X4 tropism in later disease stages, when CD4/ CCR5 T cells are limited (Joseph 2018). Thereby, co-receptor specificity is largely determined by characteristics of the V3-loop (Feed, 2001).

The entry process is one of the key steps in the HIV-1 life cycle to interfere with the host immune system and it is also the point where antibodies come into play. Neutralizing antibodies are part of the adaptive immune response that arises as early as a couple weeks after infection (Albert et al., 1990). They act for HIV by directly binding different epitopes of the envelope spike, which poses the single target for antibodies against HIV, and therefore preventing virus entry into the host cells. After successful HIV-1 infection, a person usually quickly develops a strong, neutralizing antibody response against multiple parts of Env (Wei et al., 2003). During the disease progression, HIV continuously mutates its envelope genes and thereby escapes the pressure of the antibodies (Wei et al., 2003). This viral escape can be achieved by altering of the envelope amino acid sequence, by conformation changing or through glycan shielding. Therefore, during the course of an infection, diverse patient specific and type specific antibodies evolve. In about 10-25% of all patients some broadly active, potently neutralizing antibodies that also neutralize across genetic subtypes develop after 2-3 years of infection (Gray et al., 2011 and Doria-Rose et al., 2010). In the past decades these broadly neutralizing antibodies (bnAbs) have been studied extensively as they are thought to be a fundamental component of the desired induced immune response by protective HIV vaccines (Letvin et al., 1997, Burton et al., 2012). One could already prove the potency of bnAbs in preventing and suppressing HIV-1 infection after in vivo admission (Klein et al., 2013; Burton and Mascola, 2015; Caskey et al. 2015). But still it is not totally understood under which conditions bnAbs develop (Rusert et al., 2016). Moreover, one has failed to induce a successful bnAb response comparable to the one evoked by natural infections (Burton et al., 2012).

In the year 2018, HIV had a global prevalence of 37 million people with 1.7 million new annual incidences and 770'000 million deaths [1]. In Switzerland currently 17’000 people live with HIV and in 2018 425 new incidences occurred [1]. Worldwide, 62% of all HIV infected individuals are receiving antiretroviral therapy (ART) [1, 2]. However, ART only suppresses the patient’s viral load and cannot cure HIV (Katlama et al., 2013).

As one can see from these numbers, a vaccine is greatly needed. A critical factor for developing a successful vaccine lies in the understanding of what restricts or promotes bnAb evolution in humans.

Therefore, current HIV research focuses on the questions of how a broadly neutralizing antibody response is developed and how viruses escape this pressure (Wei et al., 2003; Liao et al., 2013, McKeating et al. 1989, Frost et al., 2005). To study mechanisms of virus escape in our work we traced the evolution of envelope proteins in a patient over time. This was addressed by generation of pseudoviruses expressing an envelope protein extracted from patient plasma at six points in time. These envelopes were then characterized according to their functionality and gathered data was analysed. We expected our viruses to become more and more resistant against diverse neutralizing antibodies. Specifically, for our patient who developed broadly neutralizing antibodies against the V3 glycan epitope, we predicted changes in this region to escape the antibody pressure.

3. Methods

3.1. Patient information / Experimental setup

The Swiss HIV Cohort study (SHCS) is a nationwide, observational cohort, where patients are visited semi-annually for blood collection. It was founded in 1988 and includes 53% of all HIV and 69% of all AIDS cases in Switzerland. Within the scope of this study extensive patient and virus data as well as biobanks of plasma and blood cell samples were collected. In a recent Swiss study, named the Swiss 4.5K Screen (Rusert et al., 2016), patient samples of the SHCS were screened for determinants of bnAb induction. 4484 patients were included to examine connections between various virus, host and disease factors. Plasma samples of these patients were screened for neutralization activity. For our experiments a particularly interesting patient from the Swiss 4.5K Screen was chosen for the further exploration of viral envelope gene development. Patient ZH_5_2_13 was infected by a HIV-1 subtype B virus and found to be the 89th best neutralizer in the Swiss 4.5K Screen. His bnAbs were found to target the V3 glycan epitope best, but also the V1/V2 glycan epitope. An interesting fact regarding this patient is that he was not on ART during more than 5 years and maintained high viral load around 10'000 copies of RNA. Furthermore, the first sample was taken close to the estimated infection date, which might give the opportunity to study virus envelope genes that are preferentially transmitted. Six samples were taken over the course of almost six years. As one can observe in Figure 4, the plasma neutralization activity quite low at the beginning of the sampling and rose thereafter. In the last plasma sample, high cross neutralization activity could be detected. Each research team was assigned one sampling timepoint. The following report will focus on the analysis of latest sample 6.

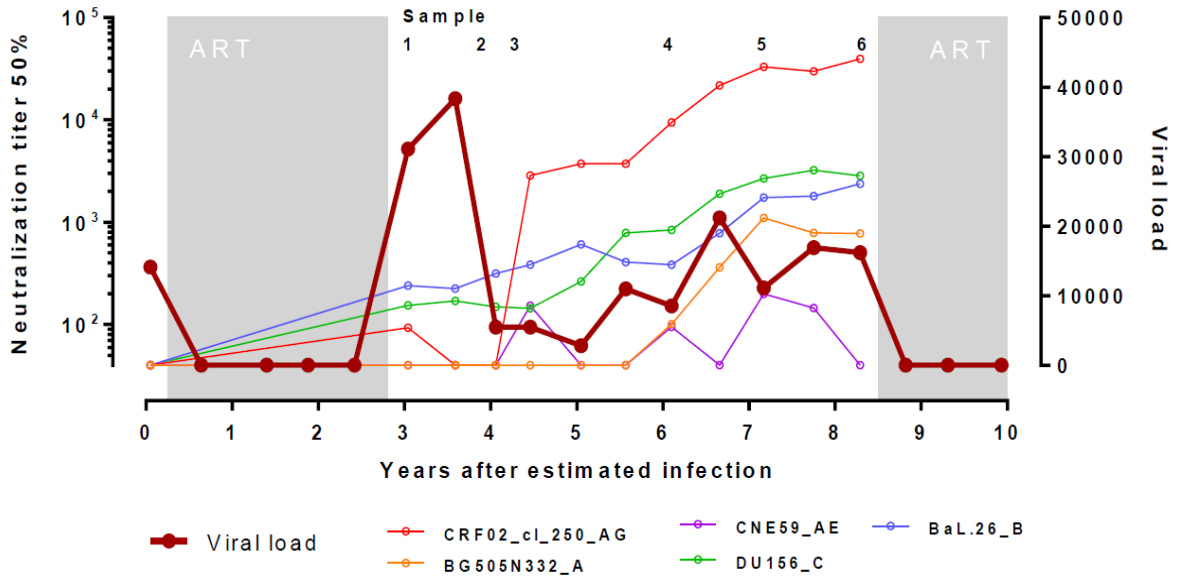

Figure 4: Disease profile of patient ZH_5_2_13. Viral load and neutralization titers are show over time, especially for the sampling timepoints (shown by numbers above). The patient was only during the grey coloured periods on ART. Figure from course script [3].

The experiments were conducted in the BL-2 and BL-3 laboratories of the Institute of Medical Virology at the University of Zurich in the context of a 3 ½ weeks block-course from the 5th Nov to the 22nd Nov 2019. Each student research group was tightly supervised by instructors being mostly PHD students. For the execution of the experiments, a course script [3] containing exact experimental setups and methods was followed. If nothing else is stated here, the experimental instructions given in the script were followed exactly and should be taken as reference. The general workflow of the steps that were performed can be seen in Figure 5. The complete experiment can be summarized as cloning of HIV-1 envelope fragments into cloning vectors, amplification of cloning vectors in plasmid cells, picking of clones, followed by extraction and purification of the envelope DNA (Chapter 3.2./4.1.). Pseudoviruses with this envelope DNA were then probed for infectivity (Chapter 3.3./4.2.), inhibition by antibodies (Chapter 3.4./4.3.), detection of cell surface envelope expression by FACS binding assay (Chapter 3.5/4.4.), and envelope sequence analysis (Chapter 3.6/4.5.).

In the following subchapters the individual steps will be described in detail one by one.

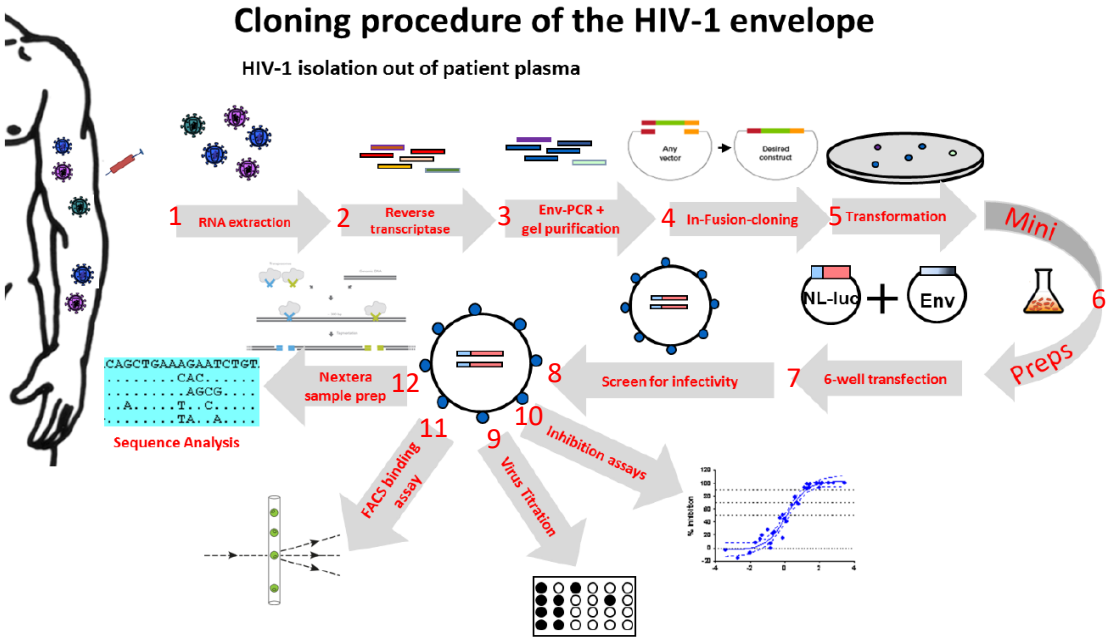

Figure 5: Schematic overview of the cloning and characterization procedure of the HIV-1 envelope. RNA was extracted from the patient and reverse transcript. The envelope fragments were then PCR amplified. The project started with the In-Fusion-cloning. Modified figure from [3].

3.2. Pseudovirus production

Before starting with the characterization of HIV-1 envelope proteins, the envelope proteins first had to be isolated and pseudoviruses carrying the proteins had to be produced. The protein isolation (Steps 1 to 3 in Figure 5) was done in advance by our instructors following the course script [3]. The first two steps were used to obtain gp160 cDNA.

RNA extraction. First, solid particles were separated by centrifugation from the patient plasma and then the RNA was extracted out of this pellet following the protocol of the “NucleoSpin RNA Virus” kit from M&N.

Reverse transcriptase of RNA. In the second step cDNA was produced from the purified RNA. This was done utilizing the "PrimeScript one Step RT-PCR Kit Vers.2 No RR055A" from Takara. Here, specific primers that anneal in conserved regions outside the envelope ORF were used in a touch down PCR to reverse transcribe RNA into cDNA and afterwards amplify this cDNA coding for the HIV gp160 protein.

PCR amplification of gp160 envelope. Step 3 of our procedure (Figure 5) was a PCR amplification of the extracted cDNA to increase the amount of envelope cDNA. This was done using the "KAPA HiFi PCR KIT" from Kapa Biosystems, which brings a KAPA HiFi DNA polymerase that replicates with a really low error rate with it. Afterwards DNA fragments were loaded onto 1% agarose gel, stained with GelRed (Chemie Brunschig), and visualized under UV light. The envelope was extracted and purified from the gel using the Qiaquick Gel Extraction Kit (Qiagen).

Unidirectional cloning of the envelope into expression vector. With this step we started our research project with the In-Fusion cloning (Step 4 in Figure 5). Using two different restrictions enzymes, the pcDNA3.1 / V5-His-TOPO (Introgen) expression vector was digested and later purified. The amplified envelope and linearized vector were combined with the In-Fusion enzyme from the In-Fusion® HD cloning KIT (Clonetec Laboratories®, Inc). A reaction without adding envelope DNA served as control. The ligation was based on the annealing of short single-stranded complementary overhangs generated by a 3'exonuclease on the vector and the insert. These overhangs were designed into the envelope PCR primers and since 3' and 5' overlaps were different, the cloning reaction was unidirectional. The cloning products were transformed into XL10 Gold chemical competent *Escherichia coli* bacteria using the heat-shock method. The transformed bacteria were plated on agar plates containing carbenicillin and incubated overnight (Step 5 in Figure 5).

Envelope plasmid amplification. Ten single colonies from the ones that had grown on the agar plates were picked and put into LB medium with carbenicillin overnight. The plasmid DNA with env insert was then purified using the Plasmid Mini-Prep Kit from Qiagen (Step 6 in Figure 5). The plasmid concentration was determined by a Nanodrop spectrophotometer, and all plasmid stocks were diluted to the same concentration for further steps.

Pseudovirus production. To probe the cloned envelope genes for functionality, the envelope plasmid and one full length HIV genome lacking the *env*-gene (also referred to as backbone) were co-transfected into HEK-293T cells. The backbone plasmid pNL-lucAM carried a firefly luciferase (luc) gene with its own SV40 promoter, which allowed the quantification of virus infectivity by measuring the enzymatic activity of luciferase in infected cells. This led to reporter gene expression in infected cells. Standard envelope expression plasmids as pcDNA3.1-JR-FL and SF162 served as positive controls, whereas pNL-lucAM was utilized as no insert control. To verify that the observed effects were HIV specific, Murine Leukemia virus (MuLV) envelope gene were transfected into 293T cells and the generated pseudoviruses were used as negative control (Step 7 in Figure 5). These generated pseudoviruses were capable of one single infection cycle, but replication incompetent, as only transcribed RNA from the backbone plasmid harboured the packaging motif and therefore the envelope-genes could not be incorporated into budding viruses. The pseudoviruses were then used for infectivity and inhibition assays, as well as for titration and envelope sequence analysis.

3.3. Virus infectivity

Infectivity screen. The generated pseudoviruses were transferred to TZM-bl cells expressing CD4 and CCR5/ CXCR4 receptors (step 8 in Figure 5). The entry inhibitor T-20 was added to half of the well-plate, serving as control for the luciferase carry-over from the 293T cells. After incubation of the mix for 48h, the medium was removed and the TZM-bl plate was prepared for the readout. Thereby, all samples were arranged on the same plate in duplicates. HIV-1 subtype B viruses JR-FL and SF162 served as positive controls, whereas Murine Leukemia virus, which should not be able to infect, was used as negative control. Upon successful infection a signal was obtained by luciferase enzyme production in the TZM-bl cells and the pseudovirus. In the TZM-bl cells this enzyme was encoded by a plasmid carrying a firefly luciferase, which got activated by the LTR of the infecting virus. The pseudoviruses carried also a firefly luciferase gene instead of their envelope gene in the backbone, which got expressed during viral replication. Luciferase enzyme production was quantified by lysis of the cells and addition of luciferase substrate. The intensity of the emitted luminescence light was measured in relative light units per microliter (RLU/µL), which translated proportionally to the HIV infection extend. The readout was performed with the Dynex MLX luminometer using the “luc med” program. Subsequent data analysis was carried out using MS Excel by the teaching assistants.

Titration assay. For the titration experiments (step 9 in Figure 5) only the most infectious pseudoviral clones from the infectivity screen were used. To determine the exact infectivity of the virus stocks we again made use of the RLU/µL method. Here, we required a linear relationship between the number of infectious particles and the readout, which in our case was the RLU signal. Using TZMI-bl cells, the association between reporter output and the HIV infection was very accurate, and therefore this criterion met. Serial 1:4 dilutions of the viral stocks were prepared, and each dilution was transferred to TZM-bl cells, where duplicates of each sample were prepared. TZM-bl cells infected with pcDNA3.1-JR-FL served as positive control. After incubation, the readout was performed similarly to the infectivity screen on the Dynex MLX luminometer, where RLU/µL were measured. Here, the data analysis was also carried out using MS Excel, where the RLU/µL values were obtained by utilizing exponential regression. Visualization of the results was done using GraphPadPrism 8.3.0.

3.4. Inhibition assay

Inhibition assay. Entry inhibition experiments were performed to assess the neutralization susceptibility of pseudoviruses carrying the envelope clones. Therefore, 4-fold serial dilutions of the antibodies PGT121 and 2G12 (V3 loop specific), VRC01 and b6 (CD4 binding site specific), 10E8 (gp41 MPER specific) and PG16 (V1/V2 loop specific) were prepared (Figure 6). Combinations of the most infectious pseudoviruses and these antibodies were incubated. These mixtures were then added to TZM-bl cells. After further incubation, the readout was performed on the Dynex MLX luminometer with the “luc med” program returning RLU/µL values.

Inhibition assay analysis. The data obtained was processed using MS Excel. We calculated inhibition activity as the reduction in infectivity, where maximum infectivity was set to the value when no inhibitor was present. We also accounted for background signal of the TZM-bl cells. Plots of inhibition curves for each inhibitor and clone combination were produced in GraphPadPrism 8.3.0. and half maximal inhibitor concentration (IC50) values were obtained from these plots.

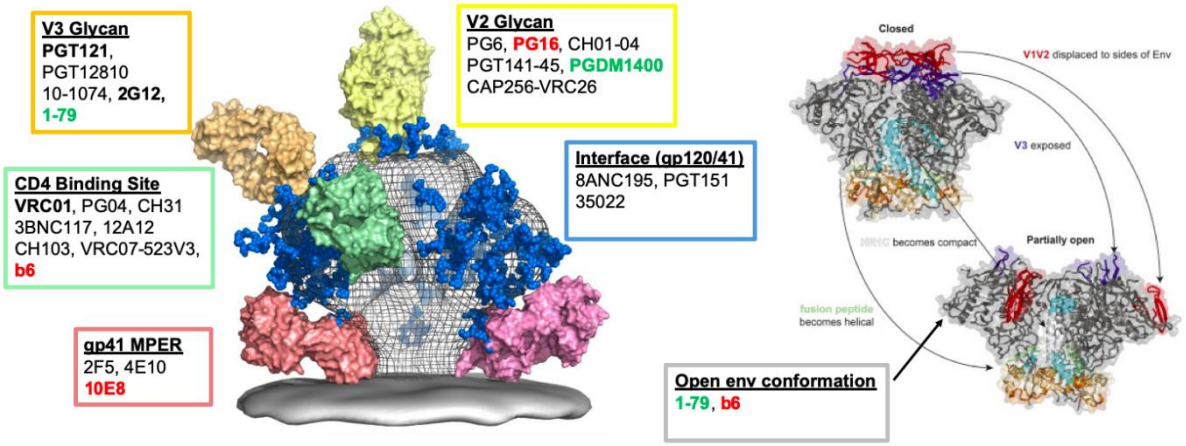

Figure 6: Target epitopes of antibodies on the HIV-1 envelope glycoprotein. Antibodies used for the inhibition assay are colored in red and bold black, whereas antibodies utilized for the flow cytometry-based assay are represented in green and bold black. Figures modified from Burton et al. (2012) and Wang et al. (2018).

3.5. Flow cytometry-based assay

FACS assay. Here, we wanted to detect the cell surface envelope expression by using a fluorescence-activated cell sorting based binding assay. Due to a tight schedule and long incubation times we were not able to take our own clones for this experiment and had to use other clones (1106-D8 and 1106-F8) obtained from the same patient at the same timepoint. 293T cells were transfected with pcDNA3.1+env together with a helper plasmid. The helper plasmid was driven by a rev1b-cytomegalovirus (CMV) promoter, which supports transgene expression of the envelope only in one direction. HIV-1 subtype B viruses pcDNA3.1-JR-FL and pcDNA3.1-SF162 served as positive controls, whereas Murine Leukemia virus (MuLV) envelope gene transfected into 293T cells served as the negative control. After incubation, the transfected 293T cells were harvested, resuspended and incubated together with primary antibodies (PGT121, 2G12, 1-79, VRC01 or PGDM1400 (Figure 6)). After washing, cells were further incubated with anti-human IgG-APC in a dark place. FACS buffer with propidium iodide was used for staining of living versus dead cells. Samples were analysed on a FACSCalibur flow cytometer with “Cellquest” software (Becton Dickinson).

FACS analysis. The binding affinities of these antibodies gave an indication of relative conformations of the envelopes. Using flow cytometry many parameters of single cells in heterogeneous cell populations could be analysed by passing them trough a laser beam cell-by-cell. From the emitted light and subsequent light scatter of each cell, cell size and granularity of single cells could be determined. The forward light scatter (FSC) is a measurement of light being scattered in forward direction and is proportional to the cell size while the side scatter (SSC) is correlated to granularity and complexity of the single cell. We analysed the data obtained by the Flow cytometry-based assay using the “Flow Jo 10.6.1” software. For the analysis, regions (gates) are drawn around desired cell populations. Those gated cells can then be further analysed or gated in additional plots. The exact gating is described in more detail in Figure 7. It is important to use the same gating for all cell populations. After sufficient gating the mean fluorescence intensity is plotted on a log scale against all

live cell counts in GraphPadPrism 8.3.0. For a positive signal we expect the histogram to look like Plot D in Figure 7, a negative signal looks like Plot F in Figure 7.

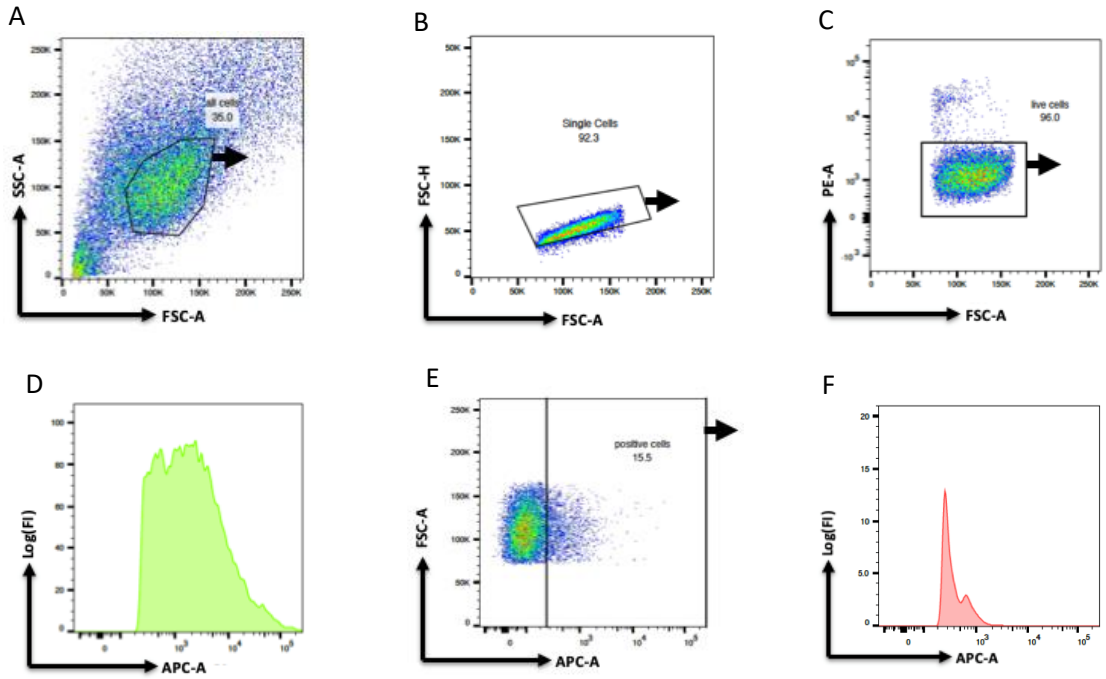

Figure 7: Gating hierarchy for sorting 293T cells. A) Dot plot of side scatter (SSC) vs. forward light scatter (FSC) to distinguish between cell populations based on size and complexity used to gate for all cells. B) Dot plot of area of the height of FSC vs. FSC to gate for single cells. C) Dot plot of propidium iodide staining vs. the area of FSC to gate for living cells. D) Histogram showing fluorescence intensity on log scale vs cell counts. E) For negative signals obtained in D, additional gating for positive cells was applied in a plot of FSC area vs. fluorescence intensity. F) Histogram of a negative signal.

3.6. Illumina sequencing

Here we wanted to know the exact sequence of the HIV-1 envelope proteins of the clones we had picked. To address this question, we used genome sequencing with the Illumina MiSeq sequencer on our most infectious clones.

Sequencing library preparation. Before getting started, a sequencing library had to be prepared. Therefore, we used the "Nextera XT kit" distributed by Illumina, specifically suited to low input amounts of DNA. The preparation consisted of tagmentation by transposomes which fragmented the Plasmid DNA and addition of a tag. This tag was then used for the annealing of primers used in the second step where through limited-cycle PCR index and adapter sequences were added. Adaptors were used to attach the fragments to flow cells and indices allowed to run multiple samples in one run and to demultiplex samples after sequencing. After various purification steps, dilution to proper concentration and pooling of multiple samples, the samples were sequenced in the Illumina MiSeq sequencer.

Sample sequencing. The Illumina MiSeq sequencer works through "Sequencing by Synthesis", meaning that at each cycle a complementary, fluorescently labelled base is added and read out. This strategy has quite low error rates and can handle reads up to 2*300 nucleotides. The output of the

device was one FASTQ file per plasmid sample. A FASTQ file is a text file consisting of four lines per read sequence, each representing a sequence identifier, the raw sequence letters, optional information about the sequence and quality values given in the ASCII format.

Envelope sequence assembly. Ending up with a mixture of short reads of the backbone plasmid and the envelope plasmid, we only wanted to retrieve the full envelope sequence. This was done in two steps. First a reference-based alignment where reads were mapped to a reference sequence of the backbone plasmids was performed using the "Smalt" algorithm. Thereby, only the backbone sequences were mapped to the reference sequence and the unaligned envelope reads extracted by "samtools" could be assembled. This was done by a de novo assembly of unaligned reads, where overlapping short reads were combined to bigger contigs using the "Velvet" assembler. All of this was done running a script performing the above-mentioned steps and outputting a FASTA file containing the assembles sequence contigs.

Sequence analysis. Further sequence analysis was done in a program called "Geneous 11.1.5". FASTA files could be imported and filtering for the longest aligned contigs was applied. Those were then mapped to the reference genome HXB2, commonly used for HIV-1. After having all sequences of all timepoints 1 to 6 (obtained by other groups) aligned, we imported them into the online webpage called "rainbow tree" [6], that compared similarities of these sequences and produced a phylogenetic tree as output. We used HXB2 as outgroup, as we assumed that it would differ most from all our clones. Furthermore, we uploaded our sequences on the online "HIV sequence database webpage" which illustrates mutations between different sequences acquiring over time.

Co-receptor analysis. The next topic we analysed was potential co-receptor switches. As mentioned in Chapter 1, all viruses in primary infections use the CCR5 co-receptor for entry whereas in 50% of the patients some viruses switch to CXCR4 during disease progression. In Chaper 1 we also stated that co-receptor specificity is largely determined by characteristics of the V3 loop. That's why by uploading the sequenced envelope genomes on the "Genafor" homepage [7], the probability of a virus using CXCR4 as coreceptor could be analysed. Therefore, the webpage used for each virus the hypothesis that this virus used CXCR4 as coreceptor and outputted a false positive rate (FPR), standing for the probability of a R5 virus being classified as X4 virus. If the FPR value returned by the program was below our cutoff of 5%, the virus was assumed to be X4 trophic.

Moreover, we wanted to confirm if the possible switches in co-receptor usage predicted by the "Genafor" homepage were actually visible through changes in the sequence of the V3 loop. There exists a 11/25 rule (Tsuchiya et al.,2013) which states that there should be changes in the 11th and 25th AA of the V3 loop upon co-receptor switch.

Glycosylation analysis. Lastly, the sequences were also checked for prominent changes in glycosylation patterns on the "HIV sequence database webpage".

4. Results

4.1. Pseudovirus production

The intent of this project was to characterize the evolution of the envelope protein in patient ZH_5_2_13 at 6 distinct sample timepoints (Figure 4), respectively the latest timepoint in case of this report. For this purpose, we generated pseudoviruses carrying the envelope fragments from sample timepoint six.

Therefore, an envelope expressing vector was required. For this purpose, the envelope fragments were cloned unidirectionally into a pcDNA3.1 / V5-His-TOPO expression vector. These cloning products were transformed into competent E.coli cells and afterwards plated to ensure single plasmid take up by the bacteria. Unfortunately, on our agar plates did not grow enough single colonies to pick from. Instead, we picked four single colonies from a premade agar plate.

For the pseudovirus production, sufficient amounts of plasmid with envelope insert were needed. For that reason, the plasmid amount was increased using bacteria. Miniprep was used to isolate the plasmid vector from the bacterial culture and the concentration of the obtained plasmid DNA was checked with a Nanotrop spectrophotometer. In our case, concentrations of clone 4 and clone 10 plasmid DNA were really low. Therefore, we exchanged both with two backup clones from the same timepoint and worked with these envelope samples.

The envelope plasmid was co-transfected with an envelope deficient HIV genome into 293T cells to create a pseudovirus. The pseudotyped viral particles were probed for functionality using an infectivity assay (Chapter 4.2.), for inhibition by antibodies using an inhibition assay (Chapter 4.3.), for detection of cell surface envelope expression by a FACS binding assay (Chapter 4.4.), and envelope sequence analysis (Chapter 4.5.).

4.2. Virus infectivity (infectivity screen and virus titration)

The pseudoviruses were used to infect TZM-bl cells, where infectivity was tested with and without the HIV entry inhibitor T20. As explained in more detail in Chapter 3.3., the method used to quantify virus infectivity relies on luciferase enzyme production, which only happens in infected cells. Infectivity of the pseudovirus clones was obtained through the intensity of emitted light measured in relative light units per microliter (RLU/µL). RLU values of all clones are presented in Table 1, where a value of 1000 RLU/µL was used as cutoff to define virus infectivity. We found that two clones, namely clone 4 and 10, clearly showed higher signals and were therefore classified as ‘infectious’. All other clones were ranked as ‘non infectious’. However, clone 9 displayed a higher RLU value compared to the remaining clones. For this reason, clones 4, 9 and 10 were used for subsequent experiments. For all wells with entry inhibitor, low RLU values could be observed. RLU values of the positive controls JR-FL and SF162 showed a similar pattern being high without T20 and low upon T20 addition. In comparison to that, the MuLV signals were always high irrespective of the presence or absence of T20.

Table 1: Infectivity capacity of the three pseudoviruses.

Group	Virus (timepoint)	Clone	Infectious?	RLU/µL	Further use
B3	#11_06	1	no	98	
B3	#11_06	2	no	92	
B3	#11_06	3	no	93	
B3	#11_06	4	yes	9274	x
B3	#11_06	5	no	119	
B3	#11_06	6	no	92	
B3	#11_06	7	no	107	
B3	#11_06	8	no	101	
B3	#11_06	9	no	409	x
B3	#11_06	10	yes	5132	x

Clones 1 to 10 from the timepoint 6 were analyzed in the infectivity screen. A cutoff of 1000 RLU/µL was used to define infectivity. Two clones, namely clone 4 and 10, were found to be infectious and were together with clone 9 used in further experiments.

As stated above, the three most infectious clones from the infectivity screen were used for virus titration. To determine the exact infectivity of the virus stocks we again made use of the RLU/µL method. By infecting TZM-bl cells with serial virus dilutions, the luciferase production was measured after 48h of incubation using the luminometer. RLU values for each dilution are shown in the Appendix (Table 2). These could be utilized to estimate RLU/µL values by exponential regression (Appendix, Figure 8). Figure 9 displays these RLU/µl values estimated for our three clones plus the control. The titration of JR-FL as the positive control, showed an infectivity value of 871.96. For clones 4 and 10 similar values of 113.85 RLU/µL, respectively 106.05 RLU/µL were obtained. Clone 9 turned out to be the least infectious with an RLU/µL value of 13.80.

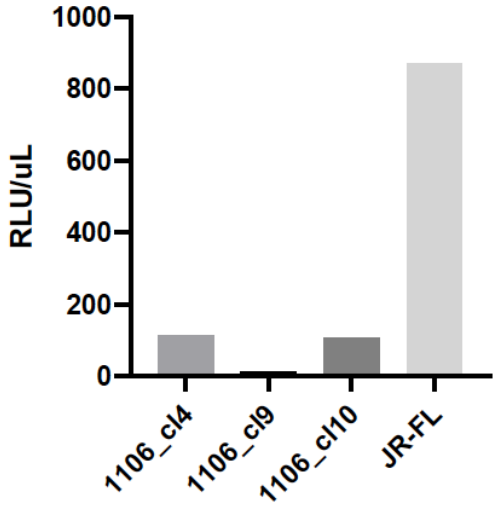

Figure 9: Results of the titration assay. RLU/µL values calculated by exponential regression from data measured in titration assay (Appendix, Figure 8/Table 2) are displayed for the three most infectious clones and JR-FL as positive control. The exact values from left to right are 113.85 RLU/µL, 13.80 RLU/µL, 106.05 RLU/µL and 871 .96 RLU/µL. Our clones were found to be less infectious than the control JR-FL, with clone 9 being the least infectious one.

4.3. Inhibition assay

To determine the effect of six monoclonal antibodies on the infection of TZM-bl cells by the infectious pseudovirus carrying the envelope clones, an inhibition assay was performed with clones 4 and 10. Here the anti-HIV antibodies PGT121 and 2G12 (V3 loop specific), VRC01 (CD4 binding site specific), b6 (CD4 binding site specific, mainly targeting open envelope conformations), 10E8 (gp41 MPER specific) and PG16 (V1/V2 loop specific) were used (Figure 6).

The inhibition assay also takes advantage of the luciferase reporter system, where inhibition activity was calculated as the reduction of infectivity. For the assay, RLU/µL values were obtained for each combination of envelope clone and antibody. The relative inhibition of the antibody was obtained by relating it to the maximal possible infection level of the non-treated virus. For comparison of the neutralization activities, each clone-inhibitor combination was visualized (Figure 10). One could observe that the curves of the combination clone 4 with 2G12, PGT121, PG16, b6, VRCO1 and clone 10 with PG16 showed a slope of zero, and therefore no inhibition capacity of the antibodies. The combination of clone 10 with 2G12, PGT121 and b6 displayed a slight increase in inhibition with increasing antibody concentrations. Nevertheless, the half maximal inhibitor concentrations (IC50) were still not reached even on high inhibitor concentration levels. On the other hand, the combination of clone 4 with 10E8 obtained an IC50 value of 0.364. Clone 10 with 10E8 showed a slightly higher IC50 value (0.512) and an even higher IC50 for VRCO1 (0.665). Thus, VRCO1 was found to be effective with one tested clone and 10E8 with both clones. All IC50 values of timepoints 2, 4 and 6 are displayed in Table 3. Generally, one could observe that the envelope clones acquired more resistance over time and the clones of timepoint 6 were found to be the overall most resistant ones.

Table 3: IC50 values clones from timepoints 2, 4 and 6.

Antibody \ Clone	0902-cl6	0902-cl1	0904-cl9	0904-cl8	1106-cl4	1106-cl10
2G12	> 20	10.21	> 20	2.78	>20	>20
VRC01	5.74	3.68	>20	5.45	>20	0.665
PG16	> 20	> 20	> 20	> 20	>20	>20
PGT121	>20	>20	>20	> 20	>20	>20
B6	13.15	2.2	> 20	> 20	>20	>20
10E8	0.0482	0.0563	1.13	0.345	0.364	0.512

Low IC50 values indicate strong the inhibition of the antibody. Values of >20 represent no inhibition observed. The antibodies 2G12 and PGT121 target the V3 Glycan epitope, VRC01 the CD4 binding site, PG16 the V2 Glycan epitope, b6 inhibits open conformations and 10E8 binds the MPER region. Clones from earlier timepoints could be inhibited better than clones of later time points. Generally, inhibition with PG16 and PGT121 did not work for any of the clones, whereas all of them could be inhibited by 10E8.

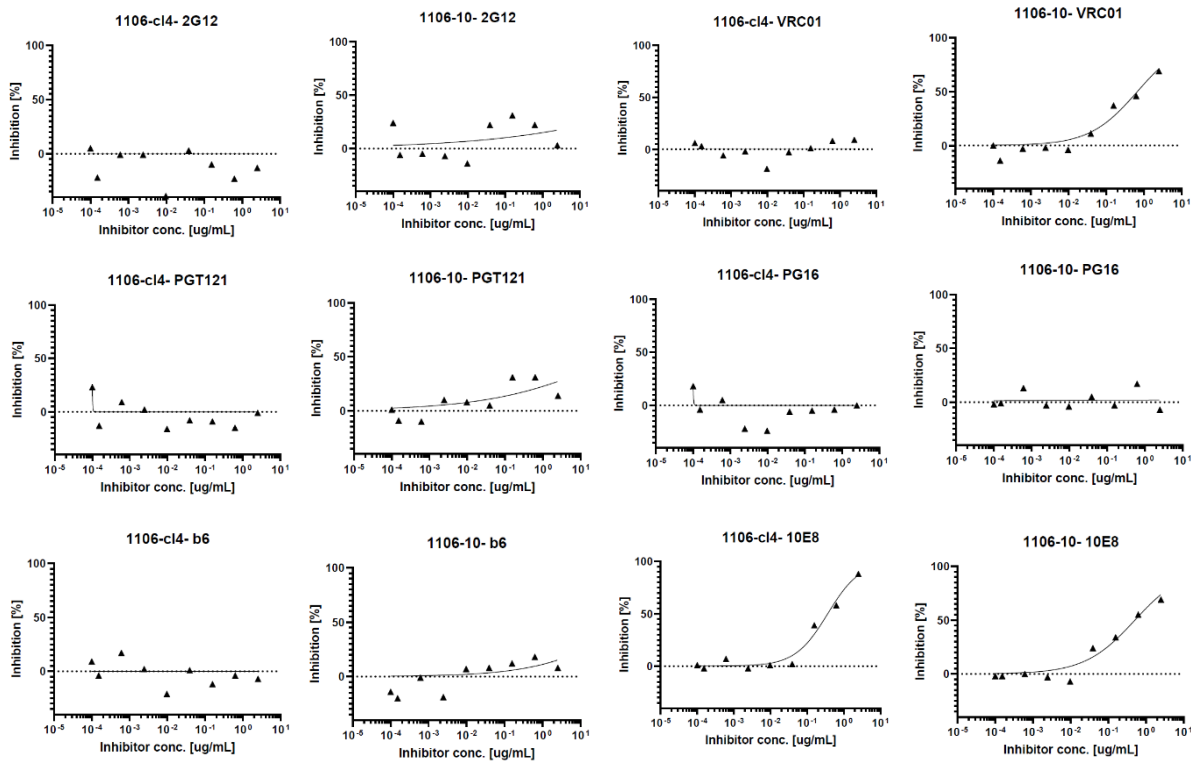

Figure 10: Inhibition assays of clones 1106-cl4 and 1106-cl10. Plots show inhibitor concentrations in µg/mL vs. relative inhibition in % for each clone/antibody combination. The antibodies 2G12 and PGT121 target the V3 Glycan epitope, VRC01 the CD4 binding site, PG16 the V2 Glycan epitope, b6 inhibits open conformations and 10E8 binds the MPER region. Apart from VRCO1 and 10E8, all antibodies failed to inhibit these two clones. VRCO1 was found to be effective with one tested clone and 10E8 with both clones.

4.4. Flow cytometry based assay

To further investigate the evolution of the viral envelope proteins, a fluorescence-activated cell sorting (FACS) based binding assay was conducted to examine the cell-surface envelope expression. For this assay two different clones (1106-D8 and 1106-F8) from the same patient and timepoint were used. The helper pCMV-rev plasmid and clones were transfected into 293T cells and in a second step these transfected 293T cells were mixed with five bnAbs. Each bnAb displayed a different epitope specificity: VRC01 is CD4 binding site specific, PGDM1400 V1/V2 loop specific and 1-79, PGT121 and 2G12 bind the V3 loop. Of these antibodies, 1-79 is known to mainly target open envelope formation [3]. During the FACS assay each cell got separately passed through the laser beam and the emitted light and light scatter were recorded by detectors. The output was gated for positive single cells using the "FlowJo 10.6.1" software (Figure 7). Histograms of fluorescence intensity for each envelope-antibody treatment are displayed in the Appendix, Figures 12-17. The median fluorescence intensity (MFI) of the envelope clones and controls were visualized for each bnAb (Figure 11), the exact values can be seen in Table 4 in the Appendix.

The FACS binding assay was not equally successful for all bnAbs. For VRCO1 and PGDM1400 both positive controls, SF162 and JR-FL, had a low mean MFI values in the range of the mean MFI values of the negative control, MuLV. On the other hand, the FACS assay control with no added antibody was successful as all envelopes displayed approximately the same signal as the negative control. Regarding

2G12 and PGT121, both clones only seemed to be a bit sensitive in comparison to JR-FL and SF162. Concerning fifth antibody, 1-79, our clones show about the same amount of signal, but we can observe decreased MFI values of the positive controls.

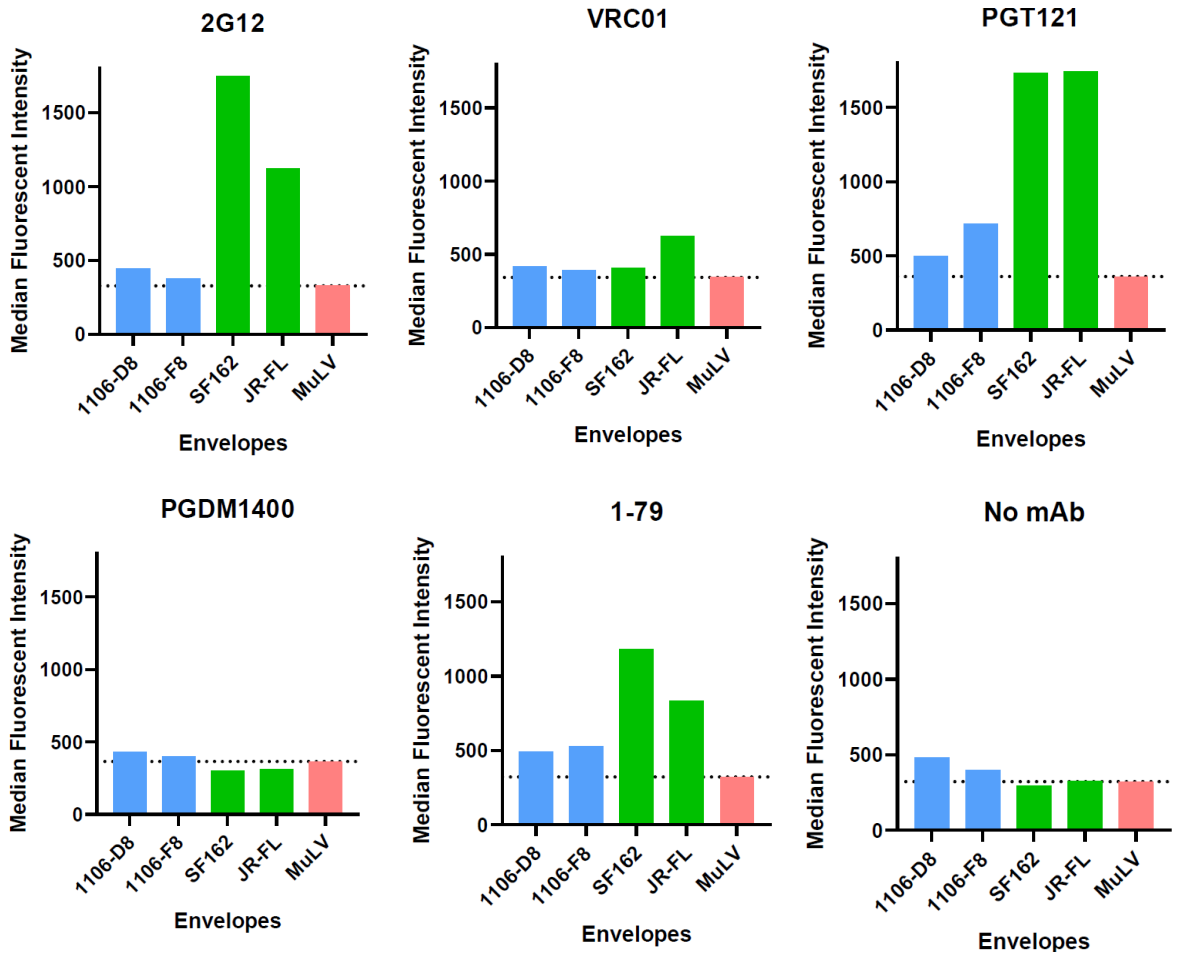

Figure 11: Median fluorescence intensity (MFI) of the FACS assay. Clones 1106-D8 and 1106-F8 are from the sampling point six, SF162 and JR-FL are positive controls and MuLV serves as negative control. The antibodies 2G12 and PGT121 bind the V3 Glycan epitope, VRC01 targets the CD4 binding site, PGDM1400 binds the V2 Glycan epitope and 1-79 inhibits open conformations. The assay seemed to have worked, as all envelopes displayed the same amount of signal as the negative control in the no mAb treatment. Both clones appear to only be a bit sensitive to 2G12 and PGT121 and more sensitive to 1-79, considering the decreased signal in the positive controls.

4.5. Illumina sequencing

To obtain the exact sequences of the HIV-1 envelope proteins of our most infectious clones 4, 9 and 10 an Illumina MiSeq sequencing approach was used. After the preparation of sequencing libraries and subsequent successful sequencing of our samples, one FASTQ file per plasmid sample was obtained. Filtering out only reads belonging to the envelope plasmid, de novo assembly of unaligned reads was utilized to obtain assembled sequence contigs. In a program called “Geneous 11.1.5”, the longest aligned contigs were then mapped to a reference genome called HXB2. In Figure 18 one can see the aligned genomes for our three clones. The different regions gp120 and gp41 are visible as well

as the variable regions illustrated with grey arrows on the sequence. We can observe that genomes of clone 9 and 10 look fine in length, whereas the genome of clone 4 seems to be a lot shorter, missing the first part of the genome.

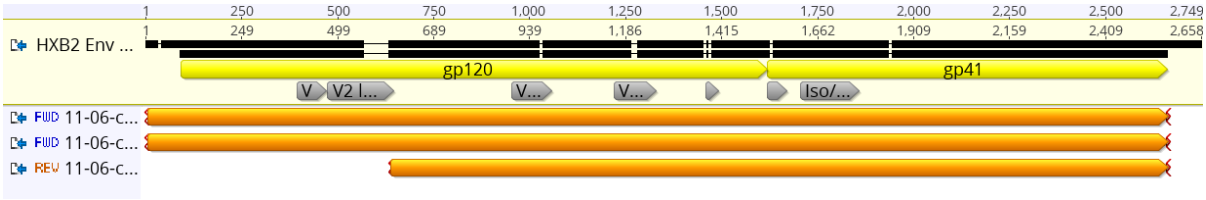

Figure 18: Aligned genomes of our three most infectious clones. HXB2 was used as reference genome and alignment was performed in 'Geneous'. Clone 4 was found to be missing the first part of its genome.

As a next step the aligned sequences of all clones from timepoints 1 to 6 were imported into the online webpage "rainbow tree" that produced a phylogenetic tree as output (Figure 19). HXB2 was again used as outgroup. We found that clones from the first sampling timepoint group together in one cluster. Moreover, clones from timepoints 2 and 3 are found together as well as 4, 5 and 6 clones. Therefore, we observed that the tree divides in early and late clones. Our two clones with a full genome (clone 9 and 10) were not found to be closest relatives, sequence 10 best fitted together with a sequence from year four, whereas sequence 9 seemed to be closely related to sequences from timepoint 5 in terms of sequence mutations.

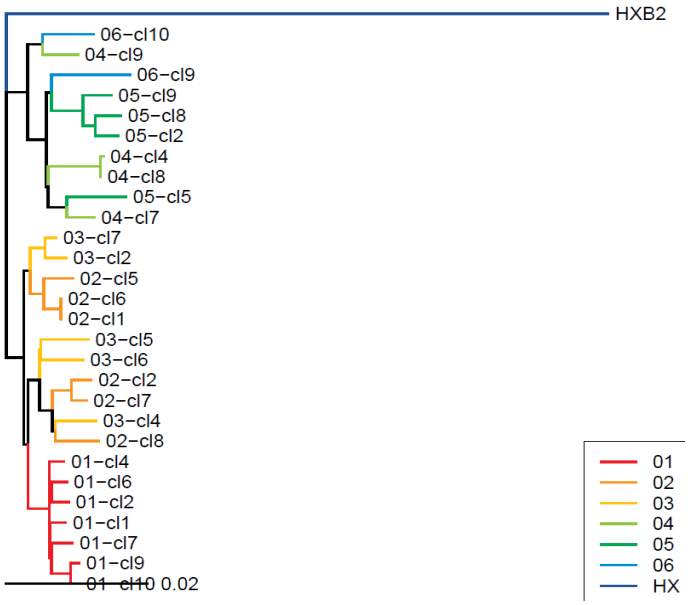

Figure 19: Phylogenetic tree of all sequenced clones. Clones from timepoints 1 to 6 were included into this phylogenetic analysis and HXB2 was used as outgroup. Clones from the first sampling timepoint were observed to group together. Furthermore, the tree splits into groups of early (timepoints 1, 2, 3) and late clones (timepoints 4, 5, 6).

Furthermore, our sequences were uploaded on the online "HIV sequence database" webpage, where mutations between different envelope sequences acquired over time were illustrated (Figure 20). For this comparison we used clone 2 from the first sampling timepoint as a reference. Mutations in comparison to this envelope genome are coloured and deletions are shown in grey. We find many mutations in the variable regions V1-V5 and the MPER region and no mutation in the signaling peptide,

which is a conserved region. Our clone 9 had the most mutations in comparison to the reference sequence, whereas clone 10 exhibited comparatively few new mutations. The ordering in Figure 20 mostly matches the grouping in the phylogenetic tree (Figure 19). Additionally, one can observe patterns in the way new mutations are acquired. There some mutations only showing up in individual clones and vanishing again afterwards. Other mutations appear at one timepoint and are then present in all following clones.

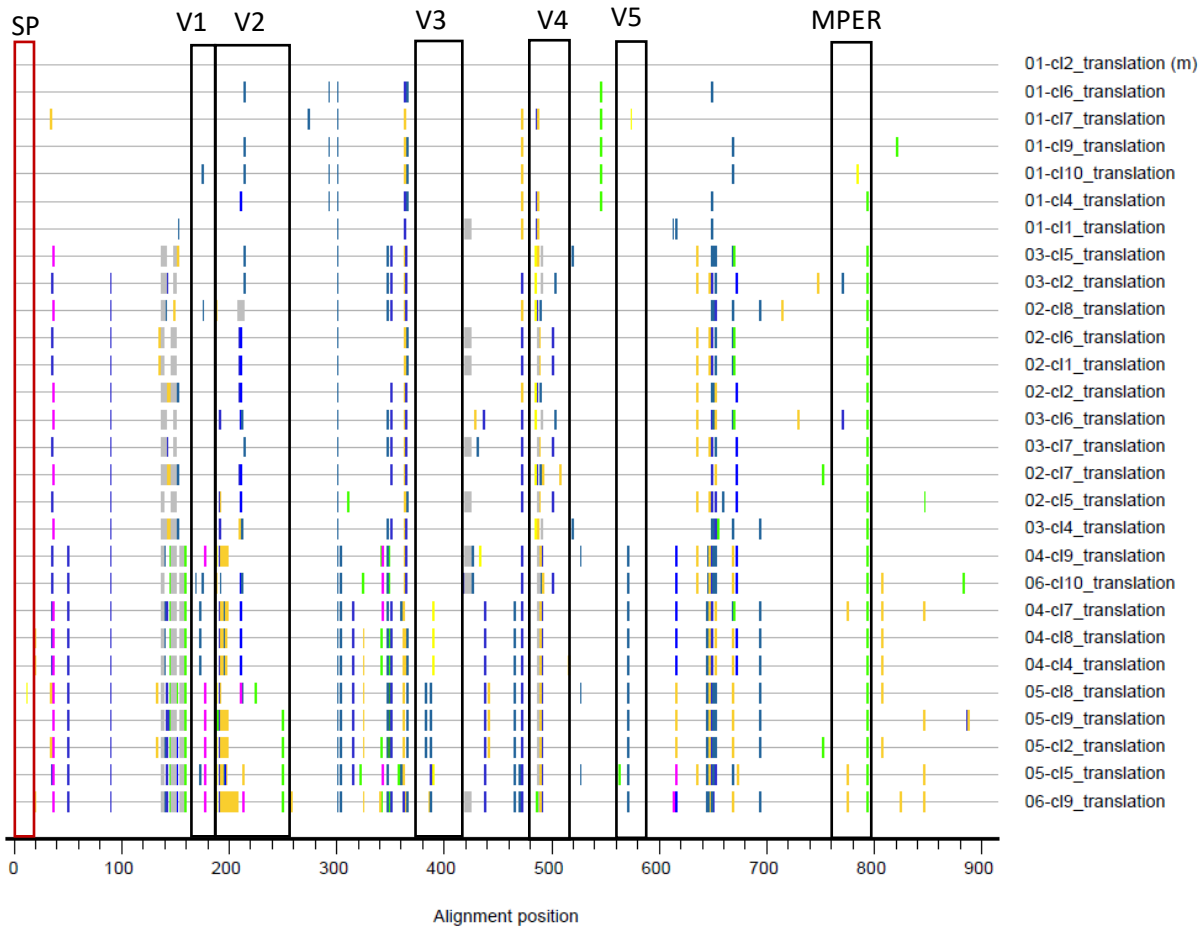

Figure 20: Differences in genome sequences between all sequenced clones. Mutations in comparison to the 01-cl2 envelope genome are coloured and deletions are shown in grey. Clones from timepoints 1 to 6 were included into this analysis. Many mutations in the variable regions V1-V5 and the MPER region can be observed and no mutation in the signaling peptide, which is a conserved region.

The next thing we investigated was co-receptor use of the envelopes. As mentioned in the introduction, all viruses in primary infection use the CCR5 co-receptor whereas in 50% of the patients some viruses switch to CXCR4 during disease progression. We also mentioned that co-receptor specificity is largely determined by characteristics of the V3 loop. By uploading the envelope genome sequences into the “Genafor” Homepage, the probability of a virus using CXCR4 as coreceptor could be analysed. Given the hypothesis that each virus uses CXCR4 as coreceptor, the output false positive rate (FPR) could be interpreted as the probability of a R5 virus being classified as X4 virus. If the FPR value returned by the program lay below our chosen cutoff of 5%, the virus was assumed to use the CXCR4 receptor. This was done for all of our clones and the resulting FPR values can be seen in Figure 21. HXB2 is a X4 trophic virus and had a FPR value of 0%. Our clones 9 and 10 from timepoint 6 were classified to be R5 trophic, as they displayed high FPR values of 91.1% and 67% respectively. Of all

analysed clones none was found to have a FPR below 5%, but two of them, namely clone 04-cl7 and 05-cl5, displayed low false positive values close to 5%.

Nr	header	V3 loop	V3 subtype	FPR
0	HXB2	CTRPNNNTRKRIRIQRGPGRAFVTIGKIGNMRQAHC	B	0%
1	06-cl9	CTRPGNNTRKSIHIGPGRTLFATGNILGDIRQAHC	B	96.1%
2	01-cl2	CTRPNNNTRKSIHIGPGRAFFATGDIIGNIRQAHC	B	83%
3	01-cl10	CTRPNNNTRKSIHIGPGRAFFATGDIIGNIRQAHC	B	83%
4	01-cl4	CTRPNNNTRKSIHIGPGRAFFATGDIIGNIRQAHC	B	83%
5	01-cl6	CTRPNNNTRKSIHIGPGRAFFATGDIIGNIRQAHC	B	83%
6	01-cl7	CTRPNNNTRKSIHIGPGRAFFATGDIIGNIRQAHC	B	83%
7	01-cl9	CTRPNNNTRKSIHIGPGRAFFATGDIIGNIRQAHC	B	83%
8	05-cl2	CTRPSNNTRKSIHIGPGRALFATGKIMGDIRQAHC	B	42.3%
9	01-cl1	CTRPNNNTRKSIHIGPGRAFFATGDIIGNIRQAHC	B	83%
10	04-cl7	CTRPNNNTRKSIHIGPGRAFYATGKIIGDIRQAHC	B	6.9%
11	04-cl8	CTRPSNNTRKSIHIGPGRALFATGNILGDIRQAHC	B	93.6%
12	04-cl4	CTRPSNNTRKSIHIGPGRALFATGNILGDIRQAHC	B	93.6%
13	05-cl5	CIRPNNNTRKSIHIGPGRAFYATGKIIGNIRQAHC	B	7.1%
14	03-cl2	CTRPNNNTRKSIHIGPGRAFFATGNIIGDIRQAHC	B	80.5%
15	03-cl6	CTRPNNNTRKSIHIGPGRAFFATGNIIGDIRQAHC	B	80.5%
16	03-cl5	CTRPNNNTRKSIHIGPGRAFFATGNIIGDIRQAHC	B	80.5%
17	02-cl8	CTRPNNNTRKSIHIGPGRAFFATGNIIGDIRQAHC	B	80.5%
18	02-cl7	CTRPNNNTRKSIHIGPGRAFFATGDIIGDIRQAHC	B	78.7%
19	02-cl2	CTRPNNNTRKSIHIGPGRAFFATGDIIGDIRQAHC	B	78.7%
20	03-cl4	CTRPNNNTRKSIHIGPGRAFFATGNIIGDIRQAHC	B	80.5%
21	05-cl8	CTRPSNNTRKSIHIGPGRAFFATGRIMGDIRQAHC	B	13.2%
22	04-cl9	CTRPNNNTRKSIHIGPGRALYATGNILGNIRQAHC	B	81.4%
23	02-cl1	CTRPNNNTRKSIHIGPGRAFFATGDIIGNIRQAHC	B	83%
24	02-cl5	CTRPNNNTRKSIHIGPGRAFFATGDIIGNIRQAHC	B	83%
25	02-cl6	CTRPNNNTRKSIHIGPGRAFFATGDIIGNIRQAHC	B	83%
26	03-cl7	CTRPNNNTRKSIHIGPGRAFFATGNIIGDIRQAHC	B	80.5%
27	06-cl10	CTRLGNNTRKSIHIGPGRAFYATGNILGNIRQAHC	B	67%
28	05-cl9	CTRPSNNTRKSIHIGPGRAFFATGRIMGDIRQAHC	B	13.2%

Figure 21: Analysis of co-receptor usage of all sequenced clones. False-positive rates (FPR) could be interpreted as the probability of a R5 virus being classified as X4 virus. A FPR value of 5% was used as cutoff for CXCR4 receptor usage. Clones from time points 1 to 6 were included into this analysis. Clones 04-cl7 and 05-cl5 exhibited a FPR value close to 5% and are therefore candidates for a possible co-receptor switch.

We looked into the position of those two clones in the phylogenetic tree (Figure 19) and they cluster together, being each other's closest predicted relatives of all clones analysed.

Moreover, the possible co-receptor switches in clones 04-cl7 and 05-cl5 were further investigated by exact analysis of the V3 loop genome sequence (Figure 22). According to the 11/25 rule, there should be changes in the 11th and 25th amino acid of the V3 loop visible upon co-receptor switch. At position 11 there were no differences between all clone envelope sequences analysed on amino acid level; all sequences had a His in comparison to the Arg found in HXB2. But at position 25 the two clones had a mutation to Lys instead of Asp / Arg observed in the other clones. HXB2 displays at this position also a lysine.

As a last part of the sequence analysis we searched for prominent changes in glycosylation patterns of the clone envelope sequences (Figure 23). A shift in glycosylation at position 332 in the V3 domain could be observed in the two clones with possible coreceptor switch. Secondly, a general pattern that could be observed was the matching of glycosylation at one position for all clones of one sampling year. These changes in glycosylation patterns match particularly between early and late clones.

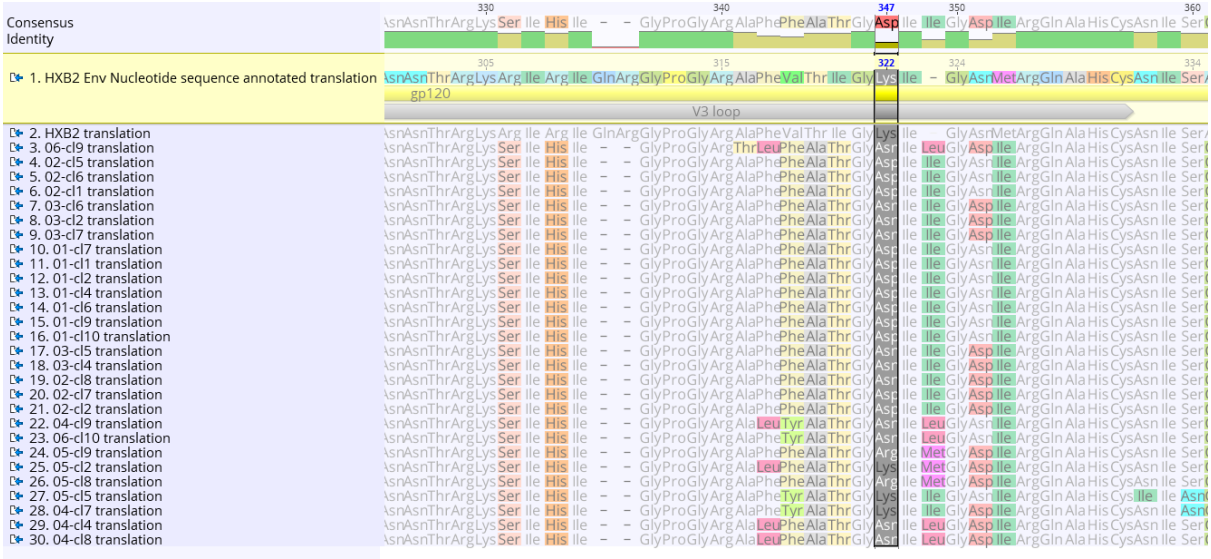

Figure 22: Sequence analysis of co-receptor usage of all sequenced clones. The 25th aminoacid of the V3-loop is highlighted in gray. Clones from timepoints 1 to 6 were included into this analysis, HXB2 used as outgroup. In co-receptor switch candidates 04-cl7 and 05-cl5, sequence analysis revealed a lysin instead of arg/asp found in other clones at position 25 of the V3-loop.

V3

Position in alignment	137	147	148	158	162	163	176	203	206	211	221	223	369	371	376	399	433	438	454	503	504	506
Hxb2 Env coordinate	130	138	139	-	149	150	160	-	-	186	-	-	332	334	339	362	-	396	411	460	461	462
Hxb2_Env(1-856)							N			N			N		N							
01-cl1	N	D	N			N		N			N		N		N	N			N			N
01-cl10	N	D	N		D	N		N			N		N		N	N	N		N			N
01-cl2	N	D	N		D	N		N			N		N		N	N	N		N			N
01-cl4	N	D	N		D	N		N			N		N		N	N	N		N			N
01-cl6	N	D	N		D	N		N			N		N		N	N	N		N			N
01-cl7	N	D	N		D	N		N			N		N		N	N	N		N			N
01-cl9	N	D	N		D	N		N			N		N		N	N	N		N			N
02-cl1		D	N		D	N		N					N		N	N			N	N		
02-cl2	N		N			N		N					N			N	N		N			N
02-cl5	N	D	N		D	N					N		N		N	N			N	N		
02-cl6		D	N		D	N		N					N		N	N			N	N		
02-cl7	N		N			N		N					N			N	N		N			N
02-cl8	N	D	N	N	D	N		N					N			N	N		N			N
03-cl2	N	D	N		D	N		N			N		N			N	N		N			N
03-cl4	N		N			N		N				N	N			N	N		N			N
03-cl5	N	D	N		N			N			N		N			N	N		N			N
03-cl6	N	D	N		D	N		N				N	N			N	N					N
03-cl7	N	D	N		D	N		N			N		N			N			N	N		
04-cl4	N	N			D	N			N		N		N		N		N		N	N		
04-cl7	N	N			D	N			N		N			N	N		N		N	N		
04-cl8	N	N			D	N			N		N		N		N		N		N	N		
04-cl9	N	N			D	N			N		N		N			N		N	N	N		
05-cl2		N				N			N		N		N		N		N		N	N		
05-cl5	N	N				N					N			N	N		N		N	N		
05-cl8		N				N						N	N		N		N		N	N		
05-cl9	N	N			D	N					N		N		N		N		N	N		
06-cl10	N	N			D	N						N	N			N		N	N			
06-cl9	N	N				N				N	N		N		N				N		N	

Figure 23: Analysis of glycosylation patterns of all sequenced clones. Only positions exhibiting differences in glycosylation between the clones are displayed, position 332/334 in the the V3-loop is highlighted. N stands for single glycosylation and D for double. Clones from timepoints 1 to 6 were included into this analysis, HXB2 used as outgroup. In co-receptor switch candidates 04-cl7 and 05-cl5, glycosylation analysis revealed a shift in glycosylation at position 332 in the V3 domain.

5. Discussion

The patient in this study provided a unique opportunity to study virus escape under antibody pressure. He had not been on ART for more than five consecutive years and maintained high viral load during that time [3] (Figure 4). Moreover, he developed a strong bnAb response, mainly against the V3 glycan epitope, but also partly against the V1/V2-loop [3]. BnAbs have been proven to prevent and suppress HIV-1 infection after in vivo admission (Klein et al., 2013; Burton and Mascola, 2015; Caskey et al. 2015). Nevertheless, up to now no successful bnAb response comparable to the one evoked by natural infections could be induced (Burton et al., 2012). In our patient, constant evolution of the viral envelope must have taken place during these five years, to keep up high viral load even under such strong antibody pressure. To research the question of how the evolution in the viral envelope had taken place, blood samples from six timepoints were compared. We hypothesized that viruses from the last timepoint would be more resistant to various bnAbs than the ones from earlier timepoints. More concretely, changes in the V3 glycan epitope were to be expected to escape the bnAb response.

We managed to produce two infectious pseudoviruses carrying an envelope from patient ZH_5_2_13 at sample timepoint six. One has to keep in mind that all our experiments were performed with a small number of pseudoviruses, which limits the significance of the results obtained.

The infectivity screen and the entry inhibition with T20 generally worked well. We can conclude this from the fact that in presence of T20, RLU values were low for all clones, as well as for JR-FL and SF162 and no change in the MuLV signal was observed when T20 was added. Furthermore, viruses were classified to be infectious if a value higher than 1000 RLU/µL was detected. The obtained signals indicated that clone 4 and 10 were infectious, whereas clone 9 was classified as being non-infectious, while probably being more infectious than the remaining other clones.

The exact infectivity of the three clones was determined in a titration assay. The infectivity of clone 4 and 10 was low in comparison to the positive control JR-FL. Additionally, the obtained value for clone 9 was even lower, matching the findings of the infectivity screen. Overall the signals were low, which can be related to the usage of 1×10^4 TZM-bl cells/well. Chen et al. (2018) demonstrated in their study that the assay sensitivity could be increased by using 4×10^4 cells/well.

Neither clone 4 nor 10 was found to be sensitive to most of the antibodies. However, both clones were effectively inhibited by 10E8. In this experimental setup, 10E8 could be seen as a positive control targeting the conserved MPER region (Oakes et al., 2019), which worked. Oakes et al. (2019) propose in their paper 10E8-like antibodies as potential anti-HIV vaccine candidates, interfering with the cell-cell fusion during the entry process. In our patient these antibodies would even have been effective at the latest timepoint. In contrast, VRCO1, targeting the CD4 binding site, was only able to inhibit clone 10. The CD4bs is quite conserved (Feng et al., 2012) and not only determined in one certain region in the genome. We could not find any mutations explaining the different susceptibility of the clones, however we propose further investigation.

Two different clones (1106-D8 and 1106-F8) from same timepoint were used in the FACS assay to detect cell-surface envelope expression. The FACS assay control, where no antibody had been added, worked successfully as all envelopes displayed approximately the same signal as the negative control. Nevertheless, the FACS assay did not work equally well for all envelope-antibody combinations.

Normally, VRCO1 is a very potent antibody [3] targeting the CD4 binding site, but in this experiment, it was only able to slightly bind to one of the positive controls, SF162. Furthermore, PGDM1400 did not attach to any envelope. Possible reasons for negative signals can be non-successful transfection, high amounts of dead cells or no luciferase expression. We obtained signals in both positive controls for other antibody combinations, which confirms that the transfection worked. In addition, specific HIV luciferase expression activation in TZM-bl cells was confirmed by the infectivity screen. However, as binding of these two antibodies did not work for other timepoints as well, we assumed that both antibodies, VRCO1 and PGDM1400, must have been degraded. The V3-glycan targeting antibodies, PGT121, 2G12 and 1-79 could all at least to some extend attach to our clones of time point six. This came as a surprise, as we assumed viruses up to timepoint six should have escaped the pressure of the V3-glycan targeting bnAbs in the patient.

Overall, much stronger binding of bnAbs to the positive controls in comparison to the envelope clones could be observed, indicating resistance in the patient's envelopes. These findings are in line with the results obtained by the inhibition assay, where two other clones from the same timepoint were as well found to be very resistant.

Sequencing of the envelope genomes of clones 4, 9 and 10, we quite surprisingly observed the genome of clone 4 to be a lot shorter than the expected 2400bp. We hypothesized the cause to be some sort of sequencing error as the clone was found to be the most infectious one in the infectivity screen. This would be highly unlikely with such a big part of the envelope genome missing. Furthermore, alignment of all sequence samples with HXB2 as outgroup resulted in a phylogenetic tree, that clustered into early (sample timepoints 01-03) and late clones (sample timepoints 04-06). The larger gap between the sampling timepoints 3 and 4 leaving more time for mutations to acquire might be a plausible explanation for these two clusters. Additionally, it is important to notice that we had more clones of the early sampling timepoints than later ones. It would have been interesting to examine if grouping of clones from timepoints 04, 05 and 06 would still be well mixed between years when more samples were added.

Moreover, we could observe mutation accumulation in the variable regions (V1-V5 and MPER) and no mutations in the conserved region (SP) over time. Additionally, we were able to observe evolutionary pressure and subsequent viral escape in the mutation patterns. At some points mutations arose in one clone and were maintained in all later clones. This led to the conclusion that the viruses had to acquire these mutations in order to escape the antibody pressure. These findings are also confirming the phylogenetic tree cluster where clusters of earlier and later clones were formed.

Regarding co-receptor usage, we expected some of the viruses to switch from CCR5 to CXCR4 as part of new escape pathways in the later timepoints. To challenge this hypothesis, the sequence of the V3-loop which largely determines co-receptor usage (Feed, 2001) was examined. Findings suggested that of all analysed clones only 04-cl7 and 05-cl5 might have undergone a co-receptor switch or transitioned to dual trophism. In these two clones, changes in the 25th amino acid position of the V3-loop could be observed, where a Lys instead of Asp / Arg found in all other clones was reported. HXB2, which is a CXCR4 using virus, also had a Lys at the same position, supporting the co-receptor switch hypothesis in these two clones. However, one would have to confirm these hypothesises with further assays.

Our findings concerning inhibition by V3-glycan specific antibodies and changes in this genome region were quite controversial. As viral loads in the patient up to the last sample were constantly high, we expected the viruses to escape the pressure of the patients bnAbs, that specifically targeted this epitope, during the course of infection. Supporting this hypothesis, we could not observe neutralization of V3-glycan specific antibodies in the inhibition assay. On the other hand, the same antibodies, PGT121 and 2G12, were found to target two other clones from the same timepoint in the FACS assay. V3-loop targeting antibodies, such as PGT121 and 2G12, are often described to be depending on glycosylation of position 332 (Sok et al., 2014). For the clones of the timepoint six no obvious changes in the genome sequences of the V3-loop as well as in glycosylation patterns could be observed. Only in two out of all clones analysed, a shift in glycosylation at position 332 could be noticed. These were the possible co-receptor switch candidates, which might have tried to escape antibody pressure in this way. However, V3-glycan specific antibodies were shown to also inhibit viruses with shifts of 332 glycosylation to position 334 (Krumm et al., 2016). Unfortunately, these two clones were not used in neither the inhibition nor the FACS assay, making any confident conclusions impossible.

In summary, we found infectious viruses to develop resistance against antibodies during disease progression, fitting our hypothesis. Results from the inhibition and flow cytometry based assay showed clones of the latest timepoint to have low susceptibility against most broadly neutralizing antibodies. In line with these findings, envelope evolution was also observed on a genetic level, where two of the clones might have undergone a co-receptor switch. Concerning the hypothesis of viral V3-glycan escape no confident statement can be made.

Having had more time for the project, we would have tested more clones of timepoint six against antibodies, particularly against V3-specific bnAbs. Additionally, we suggest resequencing of 06-cl4, as well as inhibition and FACS assays for the two co-receptor switch candidates 04-cl7 and 05-cl5. Further research examining the linkage between glycosylation shift and co-receptor usage would been interesting. Therefore, we propose co-receptor knockout/blocking in a follow-up experiment and in-depth comparison of mutations within envelopes with different bnAb responses. We furthermore suggest testing our patient's plasma against early and late clones (Albert et al., 1990) to verify autologous responses to set our findings in a broader context. Lastly, characterisation of envelope genes from another top neutralizing patient in a similar way as conducted in this study would be of great interest for comparison of envelope evolution.

The project can be seen as an explorative survey, serving as a preliminary experiment for future large-scale studies. Our results gave rise to many questions, whose answers would gain us important insight into the interplay between pressure of neutralizing antibody and viral escape. In future, a deeper understanding of HIV-1 escape pathways will be crucial for effective vaccine design.

6. Bibliography

[1] *AIDS-Hilfe Schweiz*. (2019, November). Retrieved from Statistics on HIV/AIDS: https://www.aids.ch/en/faq/hiv-and-aids/zahlen/

[2] *UNAIDS* (2019, November). Retrieved from: https://www.unaids.org/sites/default/files/media_asset/2019-UNAIDS-data_en.pdf

[3] Information was taken from the course script "Molecular Virology Course HS2019 (BIO372) – HIV-project"

[4] *The questiongene* (2019, November). Retrieved from http://questiongene.com/researching-hiv/

[5] *Wikipedia* (2019, November). Retrieved from: https://en.wikipedia.org/wiki/HIV#/media/File:HIV-genome.png

[6] *HIV Sequence database* (2019, November). Retrieved from: https://www.hiv.lanl.gov/content/sequence/RAINBOWTREE/rainbowtree.html

[7] *Genafor* (2019, November). Retrieved from: https://www.genafor.org/index.php

Albert, Jan, et al. "Rapid development of isolate-specific neutralizing antibodies after primary HIV-1 infection and consequent emergence of virus variants which resist neutralization by autologous sera." AIDS (London, England) 4.2 (1990): 107-112.

Burton, Dennis R et al. "Broadly neutralizing antibodies present new prospects to counter highly antigenically diverse viruses." Science (New York, N.Y.) vol. 337,6091 (2012): 183-6. doi:10.1126/science.1225416

Burton, Dennis R., et al. "A blueprint for HIV vaccine discovery." Cell host & microbe 12.4 (2012): 396-407.

Burton, Dennis R., and John R. Mascola. "Antibody responses to envelope glycoproteins in HIV-1 infection." Nature immunology 16.6 (2015): 571.

Caskey, Marina, et al. "Viraemia suppressed in HIV-1-infected humans by broadly neutralizing antibody 3BNC117." Nature 522.7557 (2015): 487.

Chan, David C., and Peter S. Kim. "HIV entry and its inhibition." Cell 93.5 (1998): 681-684.

Chen, Qingqing et al. "Development and optimization of a sensitive pseudovirus-based assay for HIV-1 neutralizing antibodies detection using A3R5 cells." Human vaccines & immunotherapeutics vol. 14,1 (2018): 199-208. doi:10.1080/21645515.2017.1373922

Coffin, John M., Stephen H. Hughes, and Harold E. Varmus. Retroviral Virions and Genomes— Retroviruses . Cold Spring Harbor Laboratory Press (1997)

Doria-Rose, Nicole A., et al. "Breadth of human immunodeficiency virus-specific neutralizing activity in sera: clustering analysis and association with clinical variables." Journal of virology 84.3 (2010): 1631-1636.

Feng, Yu et al. "Biochemically defined HIV-1 envelope glycoprotein variant immunogens display differential binding and neutralizing specificities to the CD4-binding site." The Journal of biological chemistry vol. 287,8 (2012): 5673-86.

Freed, Eric O. "HIV-1 replication." Somatic cell and molecular genetics 26.1-6 (2001): 13-33.

Gilbert, Peter B., et al. "Comparison of HIV-1 and HIV-2 infectivity from a prospective cohort study in Senegal." Statistics in medicine 22.4 (2003): 573-593.

Gray, Elin S., et al. "The neutralization breadth of HIV-1 develops incrementally over four years and is associated with CD4+ T cell decline and high viral load during acute infection." Journal of virology 85.10 (2011): 4828-4840.

Joseph SB, Swanstrom R. The evolution of HIV-1 entry phenotypes as a guide to changing target cells. J Leukoc Biol (2018); 103(3):421-431.

Katlama, Christine, et al. "Barriers to a cure for HIV: new ways to target and eradicate HIV-1 reservoirs." The Lancet 381.9883 (2013): 2109-2117.

Klein, Florian, et al. "Antibodies in HIV-1 vaccine development and therapy." Science 341.6151 (2013): 1199-1204.

Koff, Wayne C., and Seth F. Berkley. "The renaissance in HIV vaccine development—future directions." New England Journal of Medicine 363.5 (2010): e7.

Krumm, Stefanie A et al. “Mechanisms of escape from the PGT128 family of anti-HIV broadly neutralizing antibodies.” Retrovirology vol. 13 8. (2016)

Letvin, Norman L., et al. "Potent, protective anti-HIV immune responses generated by bimodal HIV envelope DNA plus protein vaccination." Proceedings of the National Academy of Sciences 94.17 (1997): 9378-9383.

Liao, Hua-Xin, et al. "Co-evolution of a broadly neutralizing HIV-1 antibody and founder virus." Nature 496.7446 (2013): 469.

McKeating, Jane A., et al. "Characterization of HIV-1 neutralization escape mutants." AIDS (London, England) 3.12 (1989): 777-784.

Nyamweya, Samuel, et al. "Comparing HIV-1 and HIV-2 infection: Lessons for viral immunopathogenesis." Reviews in medical virology 23.4 (2013): 221-240.

Oakes V, Torralba J, Rujas E, Nieva JL, Domene C, Apellaniz B. Exposure of the HIV-1 broadly neutralizing antibody 10E8 MPER epitope on the membrane surface by gp41 transmembrane domain scaffolds. Biochim Biophys Acta Biomembr. 2018 Jun;1860(6):1259-1271.

Pancera, Marie et al. “How HIV-1 entry mechanism and broadly neutralizing antibodies guide structure-based vaccine design.” Current opinion in HIV and AIDS vol. 12,3 (2017): 229-240.

Reeves, Jacqueline D., and Robert W. Doms. "Human immunodeficiency virus type 2." Journal of general virology 83.6 (2002): 1253-1265.

Rusert, Peter, et al. "Determinants of HIV-1 broadly neutralizing antibody induction." Nature medicine 22.11 (2016): 1260.

Sok, Devin et al. “Promiscuous glycan site recognition by antibodies to the high-mannose patch of gp120 broadens neutralization of HIV.” *Science translational medicine* vol. 6,236 (2014): 236ra63.

Tsuchiya, Kiyoto et al. “Arginine insertion and loss of N-linked glycosylation site in HIV-1 envelope V3 region confer CXCR4-tropism.” Scientific reports vol. 3 (2013): 2389.

Wang, Haoqing et al. “Partially Open HIV-1 Envelope Structures Exhibit Conformational Changes Relevant for Coreceptor Binding and Fusion.” Cell host & microbe vol. 24,4 (2018): 579-592.e4.

Watts, Joseph M., et al. "Architecture and secondary structure of an entire HIV-1 RNA genome." Nature 460.7256 (2009): 711.

Wei, Xiping, et al. "Antibody neutralization and escape by HIV-1." Nature 422.6929 (2003): 307.

7. Appendix

7.1. Results of the virus titration

Table 2: Original RLU values of virus titration.

	1106-cl4		1106-cl9		1106-cl10		JR-FL	
Undiluted	3871	8085	282	487	4431	4552	30454	33582
Dilution 1	2892	2017	232	215	2040	1746	17513	19173
Dilution 2	890	670	127	159	712	818	6809	7411
Dilution 3	290	344	146	154	436	332	2382	2558
Dilution 4	190	154	125	123	232	207	1234	1159
Dilution 5	154	121	113	123	177	144	649	526
Dilution 6	106	109	109	115	127	109	271	238
Medium only	58	58	63	65	63	52	67	67

Raw readouts (RLU values) from the luminometer. For each dilution of each virus, replicates were made. Dilutions were done on a 1:4 basis. There should be a linear relationship between the readout and virus concentration, which is mostly true only for the first couple of dilutions. The readout of the high dilutions are noisy in the range of the background noise (medium only).

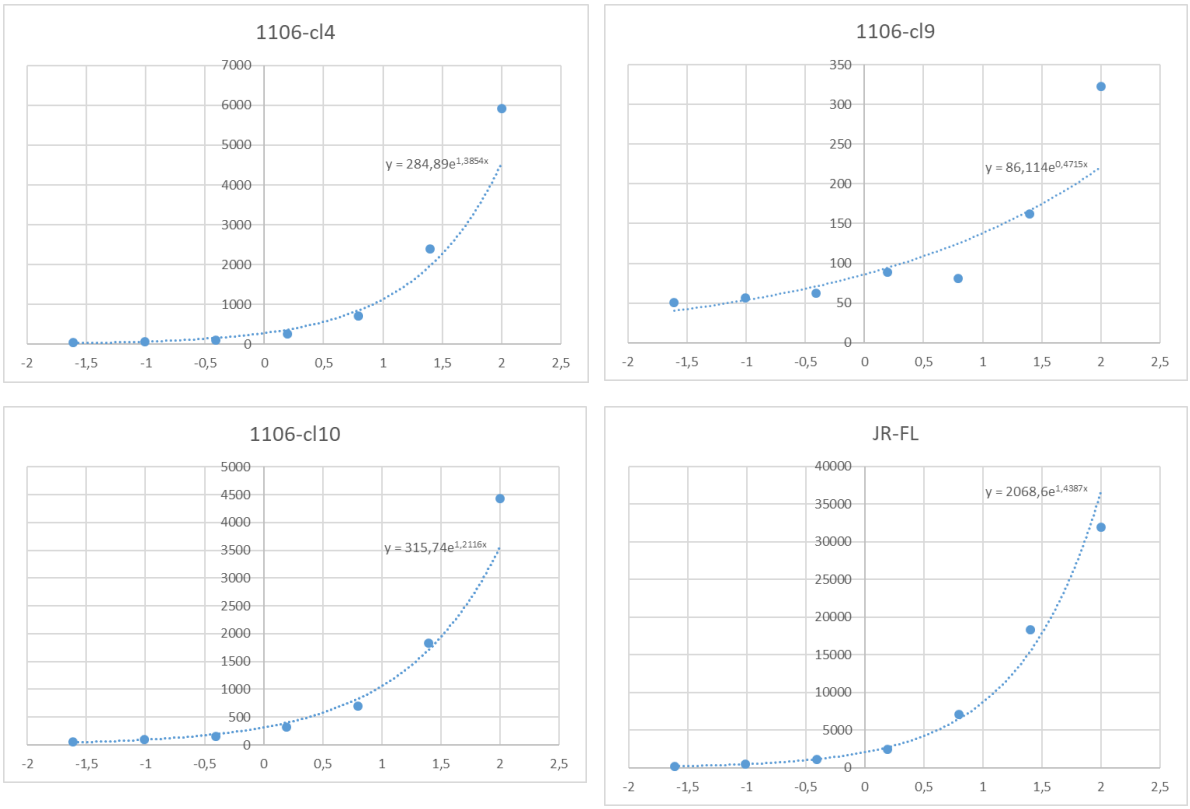

Figure 8: Exponential regression of virus titration. RLU values represented in Figure 7 were averaged, mean background values substracted and then plotted against the log virus concentration. The fit was relatively well for all four titrations. From the estimated exponential regression graphs RLU/µL values of 113.85, 13.80, 106.05 and 871 .96 could be obtained for clones 4, 9, 10 and JR-FL.

7.2. Results of the FACS assay

Table 4: Median fluorescence intensity (MFI) values obtained by the FACS assay.

Antibody \ Clone	1106-D8	1106-F8	MuLV	JRFL	SF162
2G12	443	379	328	1120	1748
VRC01	416	392	342	625	406
PGT121	499	715	361	1740	1732
PGDM	431	401	365	312	302
1-79	489	527	322	834	1181
no Ab	479	398	321	323	296

Displayed are the results of clones 1106-D8 and 1106-F8 from the sampling point 6, SF162 and JR-FL being positive controls and MuLV serving as negative control. The antibodies 2G12 and PGT121 bind the V3 Glycan epitope, VRC01 targets the CD4 binding site, PGDM1400 binds the V2 Glycan epitope and 1-79 inhibits open conformations. The FACS binding assay was not equally successful for all bnAbs. We find only a little signal for the clones D8 and F8 in combination with the antibodies 2G12 and PGT121. Additionally we observe the clones to be a little more sensitive to 1-79, accounting for the lowered response in the positive controls.

FACS assay of 2G12

Env 1106-D8: positive cells: 1741

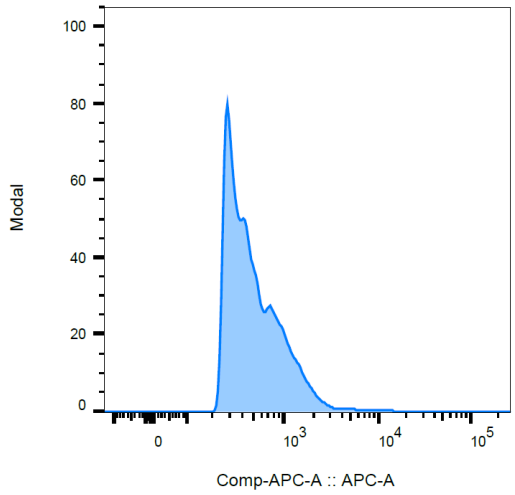

Env 1106-F8: positive cells: 948

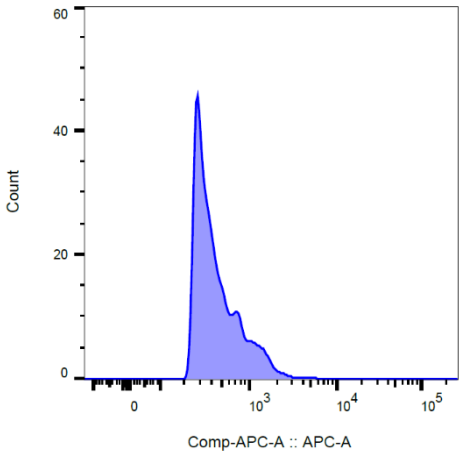

Positive Control JRFL: positive cells: 4771

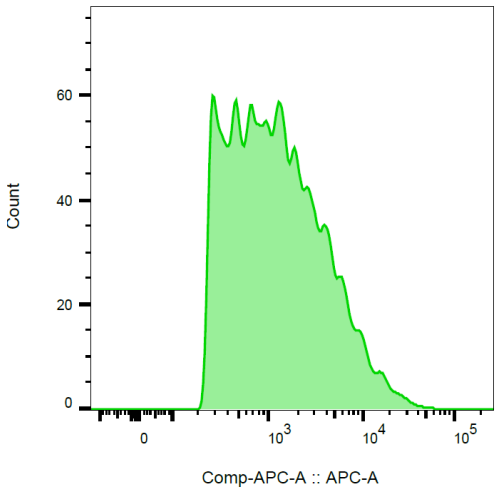

Positive Control SF162: positive cells: 9115

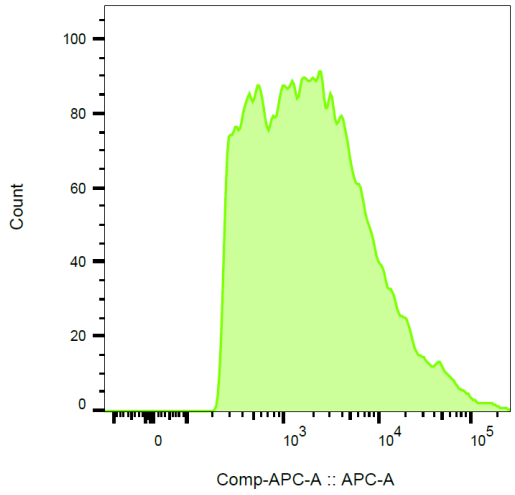

Negative Control MuLV: positive cells: 219

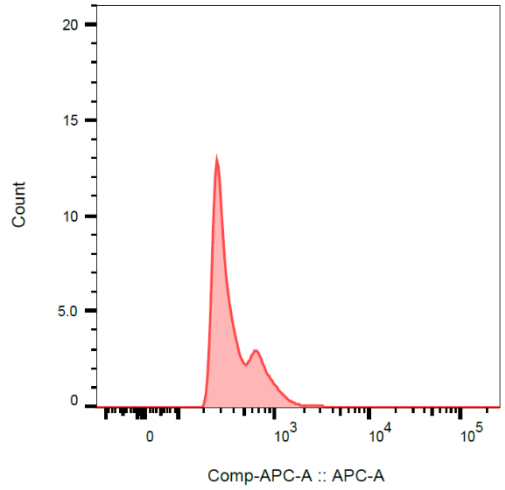

Figure 12: Results of the FACS assay of the antibody 2G12. Clones 1106-D8 and 1106-F8 are from the sampling point six, SF162 and JR-FL are used as positive controls and MuLV served as negative control. The antibody 2G12 binds the V3 Glycan epitope. Both clones only seemed to be a bit sensitive to 2G12 in comparison to the positive controls JR-FL and SF162.

FACS assay of VRC01

Env 1106-D8: positive cells: 2196

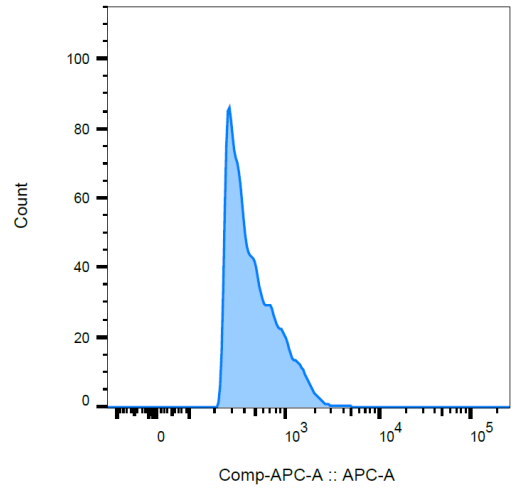

Env 1106-F8: positive cells: 2494

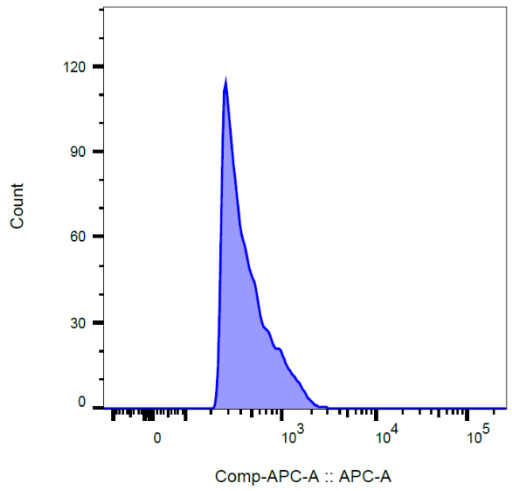

Positive Control JRFL: positive cells: 3355

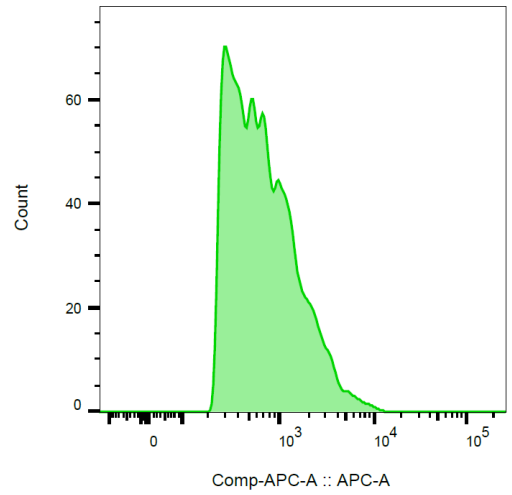

Positive Control SF162: positive cells: 3238

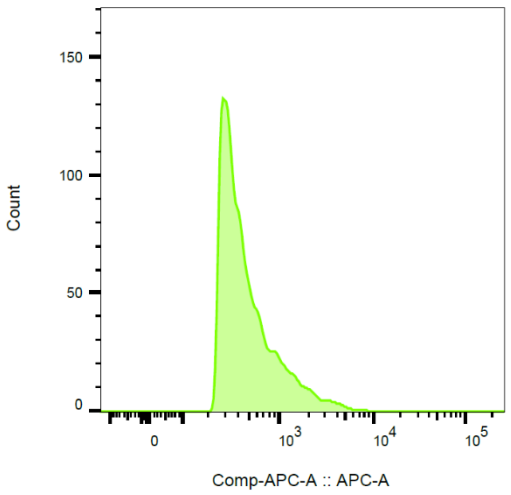

Negative Control MuLV: positive cells: 240

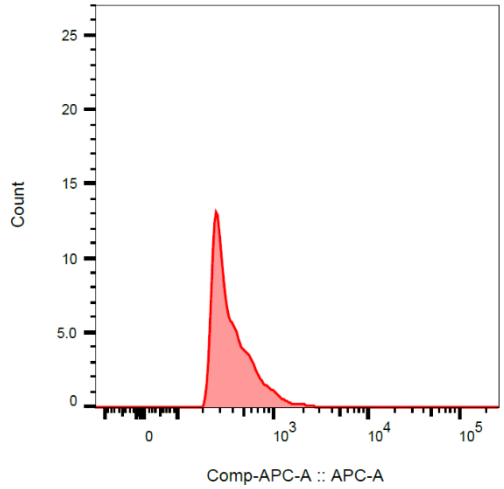

Figure 13: Results of the FACS assay of the antibody VRCO1. Clones 1106-D8 and 1106-F8 are from the sampling point six, SF162 and JR-FL are used as positive controls and MuLV served as negative control. The antibody VRC01 targets the CD4 binding site. The FACS assay for VRCO1 seems not to have worked properly as both positive controls, SF162 and JR-FL, had a low mean MFI values in the range of the mean MFI values of the negative control.

FACS assay of PG121

Env 1106-D8: positive cells: 5186

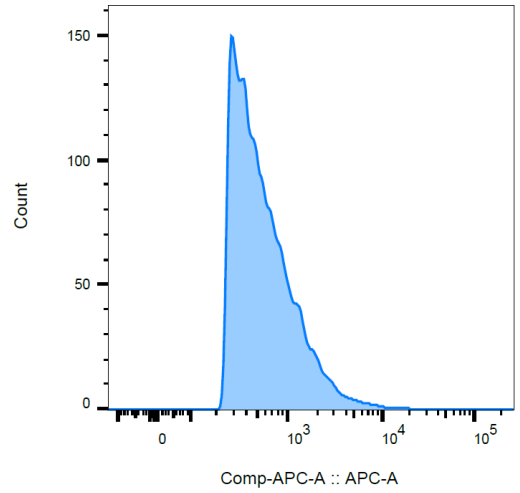

Env 1106-F8: positive cells: 7778

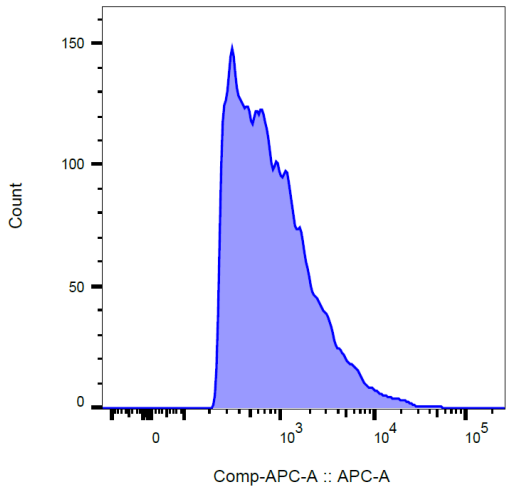

Positive Control JRFL: positive cells: 8977

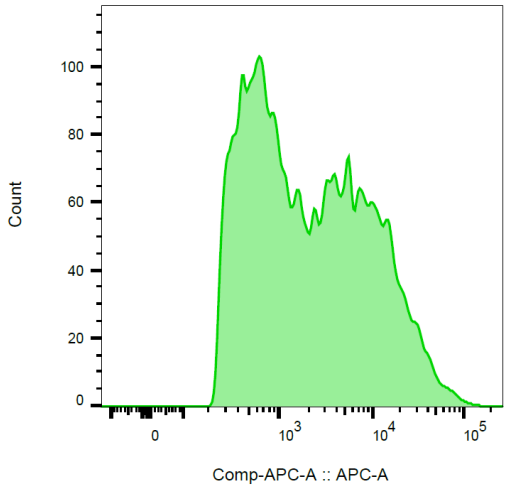

Positive Control SF162: positive cells: 9893

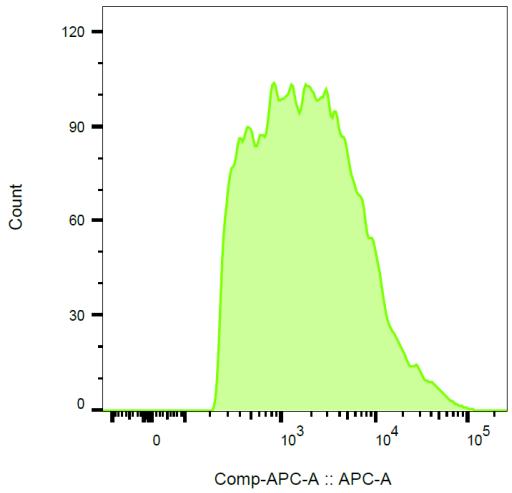

Negative Control MuLV: positive cells: 264

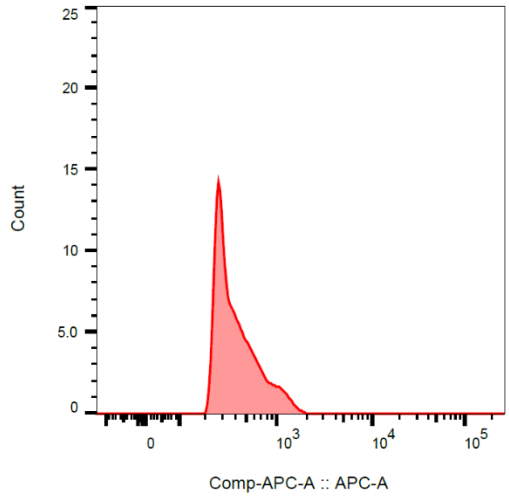

Figure 14: Results of the FACS assay of the antibody PGT121. Clones 1106-D8 and 1106-F8 are from the sampling point six, SF162 and JR-FL are used as positive controls and MuLV served as negative control. The antibody PGT121 binds the V3 Glycan epitope. Both clones only seemed to be a bit sensitive to PG121 in comparison to the positive controls JR-FL and SF162.

FACS assay of PGDM1400

Env 1106-D8: positive cells: 1366

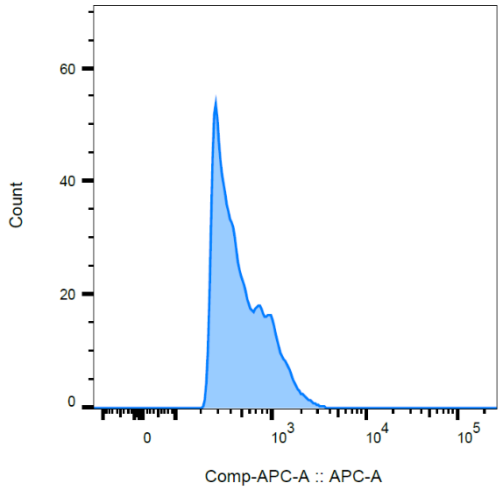

Env 1106-F8: positive cells: 1189

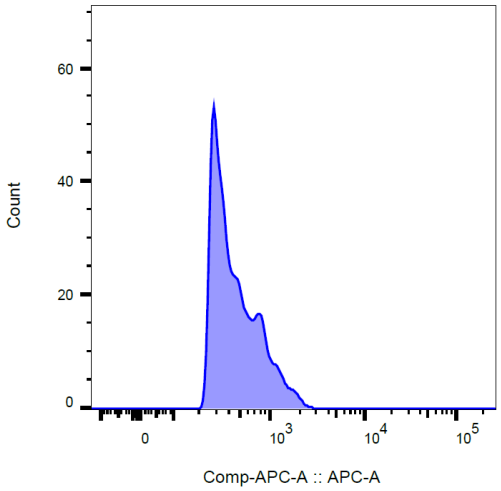

Positive Control JRFL: positive cells: 589

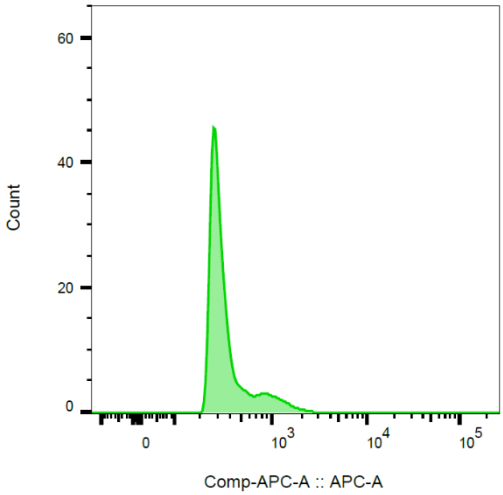

Positive Control SF162: positive cells: 437

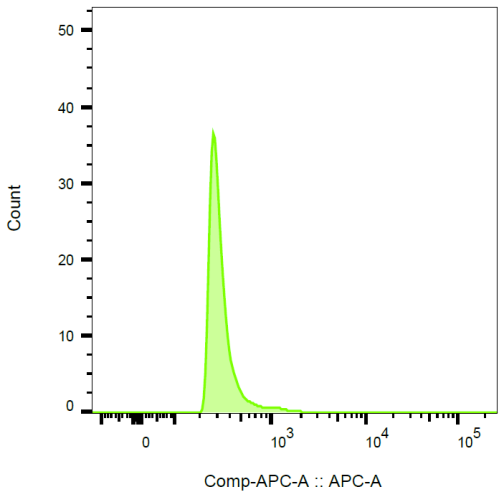

Negative Control MuLV: positive cells: 197

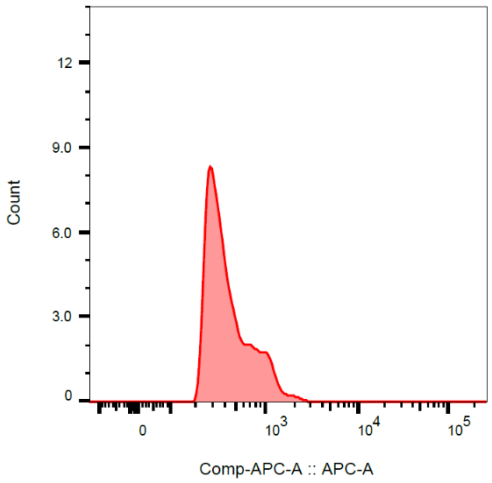

Figure 15: Results of the FACS assay of the antibody PGDM1400. Clones 1106-D8 and 1106-F8 are from the sampling point six, SF162 and JR-FL are used as positive controls and MuLV served as negative control. The antibody PGDM1400 binds the V2 Glycan epitope.
The FACS assay for PGT1400 seems not to have worked properly as both positive controls, SF162 and JR-FL, had low mean MFI values in the range of the mean MFI values of the negative control.

FACS assay of 1-79

Env 1106-D8: positive cells: 4536

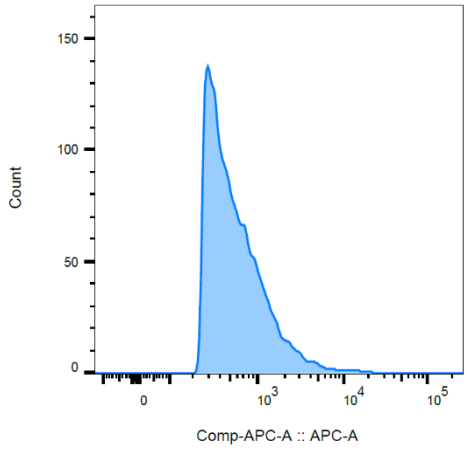

Env 1106-F8: positive cells: 5987

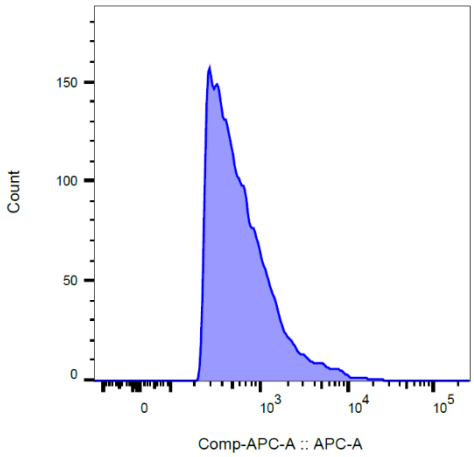

Positive Control JRFL: positive cells: 5118

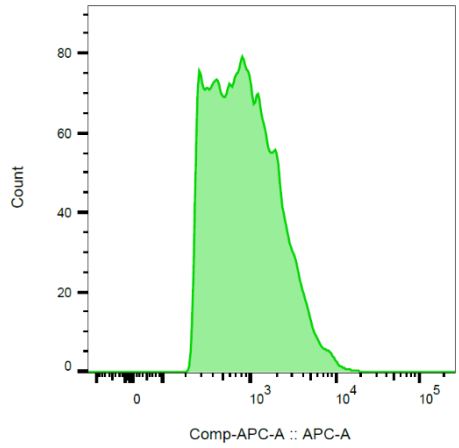

Positive Control SF162: positive cells: 8941

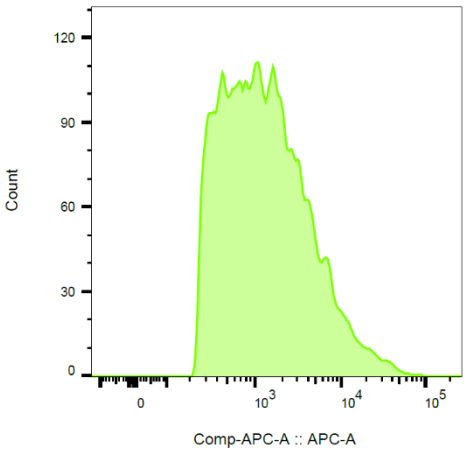

Negative Control MuLV: positive cells: 214

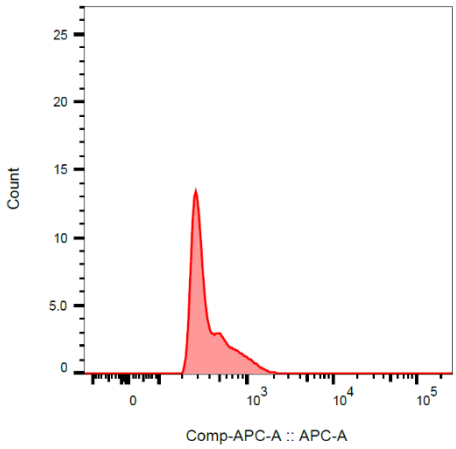

Figure 16: Results of the FACS assay of the antibody 1-79. Clones 1106-D8 and 1106-F8 are from the sampling point six, SF162 and JR-FL are used as positive controls and MuLV serves as negative control. The antibody 1-79 inhibits open conformations. The clones D8 and F8 show some signal, which we can interpret as positive signal considering decreased MFI values for the positive controls.

FACS assay no Antibody

Env 1106-D8: positive cells: 1134

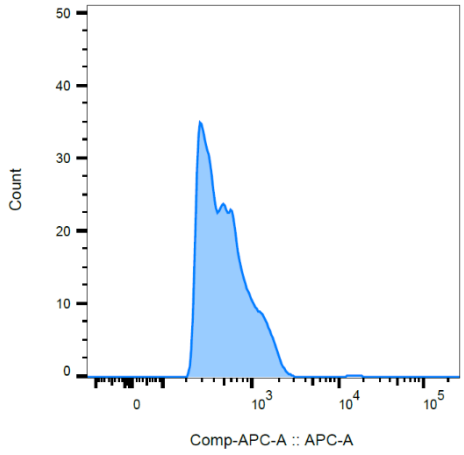

Env 1106-F8: positive cells: 430

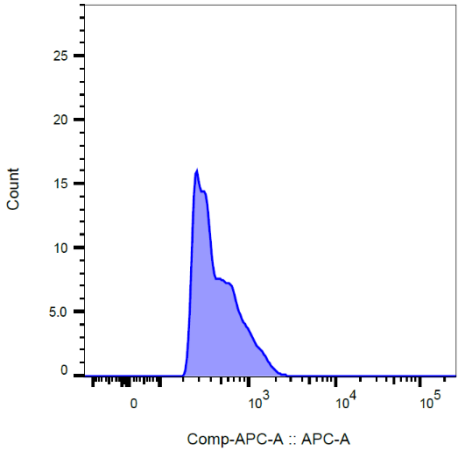

Positive Control JRFL: positive cells: 229

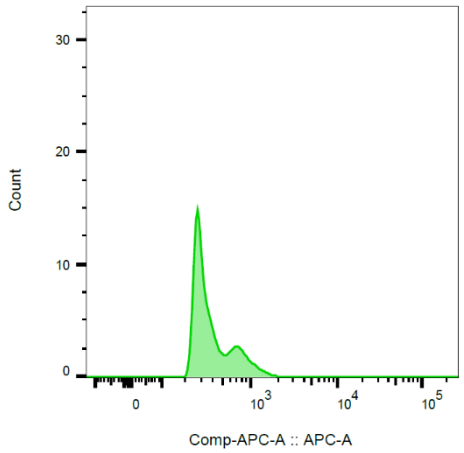

Positive Control SF162: positive cells: 457

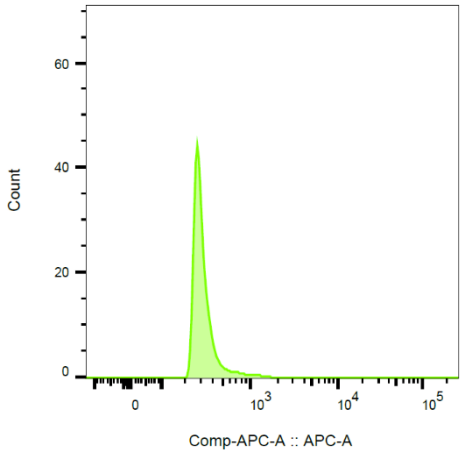

Negative Control MuLV: positive cells: 249

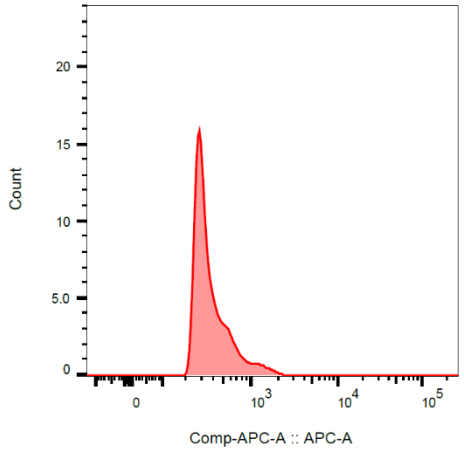

Figure 17: Results of the FACS assay with no antibody treatment. Clones 1106-D8 and 1106-F8 are from the sampling point six, SF162 and JR-FL are used as positive controls and MuLV serves as negative control. Here, no antibody was used. The FACS assay control with no added antibody was successful, as all envelopes displayed approximately the same signal as the negative control.